Mathematical Biosciences and Engineering

https://www.aimspress.com/journal/mbe

MBE, 23(7): 2132–2177.
DOI: 10.3934/mbe.2026078
Received: 11 April 2026
Revised: 24 May 2026
Accepted: 04 June 2026
Published: 15 July 2026

Research article

Mathematical analysis of a vector model using larvicides and *Wolbachia*-infected male mosquitoes: an optimal and impulsive control approach

Wendpanga Birba[1], **Boureima Sangaré**[1,*] **and Abdoulaye Kaboré**[1,2]

[1] Laboratoire de Mathématiques Informatique et Applications (LaMIA), Université Nazi BONI, 01 BP 1091, Burkina Faso

[2] Université Lédéa Bernard Ouédraogo, 01 BP 346 Ouahigouya 01, Burkina Faso

* **Correspondence:** Email: mazou1979@yahoo.fr.

Abstract: In this paper, we develop and analyze a mathematical model for mosquito population control, incorporating the release of *Wolbachia*-infected male mosquitoes and the application of larvicides. Two complementary approaches are considered: An optimal control model with continuous-time control functions, and an impulsive control model accounting for periodic releases of *Wolbachia*-infected male mosquitoes and larvicide. The main objective is to minimize the population of fertilized females, which are responsible for the transmission of vector-borne diseases, while reducing the associated biological, social, and economic costs. Using the Pontryagin maximum principle, we characterize the optimal controls and demonstrate the existence of admissible solutions. Within the framework of the impulsive model, the existence and stability conditions for periodic solutions are rigorously derived, allowing the identification of critical thresholds for the larvicide concentration and the minimum density of *Wolbachia*-infected mosquitoes required to achieve a significant reduction in the target population. Numerical simulations illustrate the enhanced effectiveness of the combined intervention strategy, demonstrating both faster response times and a greater impact on population suppression. These findings emphasize the necessity of a scientifically grounded, optimized, and integrated approach in the design and implementation of vector control programs.

Keywords: mathematical model; optimal control; Pontryagin maximum principle; impulsive control; *Wolbachia*; numerical analysis

1. Introduction

Vector-borne diseases remain among the leading causes of global morbidity and mortality, affecting over 80% of the world's population annually, particularly in tropical and subtropical regions [1, 2]. Cli-

mate change, land-use alterations, and increasing global trade are expected to exacerbate the prevalence of these diseases in the coming decades [3]. In this context, mosquitoes, which are primary vectors of the pathogens responsible for malaria, dengue, chikungunya, and zika, pose a growing threat to public health. In the absence of effective vaccines for many of these diseases, the most reliable strategy for preventing transmission remains the reduction or elimination of vector mosquito populations [4, 5]. However, conventional vector control methods, which largely rely on insecticide use, face significant limitations: The emergence of insecticide resistance, the high cost of repeated treatment campaigns, environmental pollution, and non target impacts on ecosystems [6]. As a result, innovative biological alternatives are being developed, notably the sterile insect technique (SIT) and the incompatible insect technique (IIT), the latter of which involves introducing a naturally occurring intracellular bacterium of the genus *Wolbachia* into wild mosquito populations [7–9].

Indeed, SIT, first introduced in the 1950s by Bushland and Knipling, involves releasing large numbers of sterilized males to reduce the reproductive success of wild populations. IIT exploits the ability of *Wolbachia* to induce cytoplasmic incompatibility, whereby mating between infected males and uninfected females results in non viable offspring. Additionally, *Wolbachia* has been shown to reduce the vector competence of mosquitoes for viruses such as dengue [8, 10]. Since 2011, initiatives such as the World Mosquito Program have implemented field releases of *Wolbachia*-infected *Aedes aegypti* mosquitoes in various countries (e.g., Indonesia, Vietnam, Australia), demonstrating promising reductions in dengue's incidence [11]. Nonetheless, field outcomes have exhibited considerable variability across ecological settings. In cities such as Medellín (Colombia) and Rio de Janeiro (Brazil), the establishment rates of *Wolbachia* in local mosquito populations have remained low, despite sustained release efforts [12]. These findings highlight the importance of tailoring deployment strategies to specific environments and the need for mathematical tools to better understand intervention dynamics and optimize implementation protocols.

In this regard, mathematical modeling, combined with optimal and impulsive control theory, provides a robust framework to assess, simulate, and optimize vector control strategies. These approaches account for complex biological population dynamics, operational constraints, and economic considerations. Several studies have shown the value of such models in improving the deployment of innovative control methods [13, 14]. For instance, optimal control models have been used to determine the minimal intervention effort needed to reduce fertile female mosquito populations, considering the costs related to larvicide application, production of sterile or infected mosquitoes, and disease burden [15–18]. The use of *Wolbachia* has been especially well studied in this context. Ferguson et al. [15] demonstrated that optimizing the timing and scale of mosquito releases can significantly enhance the intervention's efficacy, while Bliman et al. [19] developed intervention models minimizing the number of insects released without the need for continuous field surveillance. Furthermore, impulsive control approaches have been proposed to model the effects of discrete, periodic releases, identifying optimal release frequencies and intensities [20–23].

In particular, the foundational work of Kabore et al. [24] established a critical baseline by analyzing mosquito population dynamics under constant and periodic releases of *Wolbachia*-infected males, deriving important thresholds such as the critical release size M_i^{crit} and the basic offspring number $\mathcal{N}$. However, their study considered larvicide application only as a constant mortality term and did not integrate it as a dynamic, optimizable control variable. Furthermore, while they analyzed periodic releases, they did not formulate or solve an optimal control problem to dynamically adjust both larvicide

applications and male releases in response to population changes over time. These limitations restrict the model's ability to inform cost-effective, adaptive, and integrated field strategies that combine chemical and biological controls under realistic operational constraints. More recently, Ma et al. [25] developed a spatial partial differential equation (PDE) model to investigate barrier strategies using the SIT alone. While their work provides valuable insights into the spatial invasion dynamics, it does not incorporate dynamic optimization, nor does it combine multiple control interventions. Unlike [24], where (i) larvicide is modeled as a constant parameter, (ii) *Wolbachia*-infected male releases are imposed exogenously (constant or periodic), and (iii) no dynamic optimization is considered, the present work introduces a unified dual-control framework in which both larvicide and male releases are treated as time-dependent decision variables. Moreover, in contrast to [25], which focuses on a single intervention (SIT) within a spatial framework, our work is temporally focused but integrates two distinct interventions (larvicide and *Wolbachia*-infected male releases) within a unified optimization framework. This approach not only allows us to formulate and solve an optimal control problem, but also captures the impulsive nature of real-world interventions and identifies critical thresholds governing the long-term suppression of the vector population. In addition, *Wolbachia* induces cytoplasmic incompatibility (CI), whereby early embryos die when wild females mate with infected males. When this embryonic mortality is total, the phenomenon is referred to as complete CI; otherwise, it is termed incomplete CI. It should be noted that the present study focuses exclusively on the case of complete CI.

This study then significantly extends the framework of [24] by developing a novel integrated vector control strategy that combines the release of *Wolbachia*-infected male mosquitoes with larvicide application within a unified dual-control mathematical framework. Unlike previous works, our work introduces two complementary modeling approaches.

- A continuous-time optimal control model that determines time-varying strategies for larvicide application and male releases to minimize both the epidemiological impact and the economic cost. Unlike the threshold-based analysis of [25], our optimal control formulation uses Pontryagin's maximum principle to dynamically adjust both intervention's intensities in response to population changes.
- An impulsive control model that explicitly incorporates the larvicide concentration as a decaying state variable and periodic male releases, capturing the discrete nature of field interventions more realistically.

The main mathematical contributions of this study are as follows.

- The rigorous derivation of time-dependent optimal control strategies using Pontryagin's maximum principle, providing a theoretical foundation for designing interventions that balance epidemiological impact with economic cost.
- The identification of biologically meaningful threshold values, such as the critical larvicide concentration (L^{crit}) and the minimum release size of *Wolbachia*-infected males (M_i^{crit}), which are necessary to achieve long-term suppression of the wild mosquito population. Beyond the critical release size identified in [24] and the barrier thresholds in [25], we also identify the critical larvicide concentration L^{crit} and the frequency thresholds τ_1^*, providing operational guidance for integrated vector management.
- The analytical demonstration of existence and stability of periodic solutions within the impulsive control model using Floquet theory and perturbation analysis, offering insights into the long-term

dynamics of mosquito populations under discrete interventions.

- Numerical simulations that validate the theoretical findings and reveal the synergistic effects of combining chemical and biological controls, showing that integrated strategies can achieve more than a 90% reduction in the population of fertilized female mosquitoes.

The rest of the article is organized as follows: After the introduction, Section 2 provides a brief overview of the base model. Section 3 develops our optimal control model, considering two types of controls: The application of larvicides and the continuous release of *Wolbachia*-infected male mosquitoes. We study the existence of controls and characterize the optimal control problem. Section 4 is dedicated to the development of the impulsive control model, where the concentration of larvicides is treated as a system variable and where the release of *Wolbachia*-infected male mosquitoes occurs periodically. We analyze the boundedness of the solutions and the existence of periodic equilibria, and determine the thresholds for larvicide concentration and the quantity of infected male mosquitoes. Section 5 presents the results of the numerical simulations for both models. Finally, the conclusion is given in Section 6.

2. Foundational model for mosquito population dynamics

In this section, we recall the mathematical model previously introduced in [24], which serves as the foundational framework for our current study. That original model consists of a system of nonlinear ordinary differential equations (ODEs) designed to evaluate the effects of releasing *Wolbachia*-infected male mosquitoes, alongside mechanical control and larvicidal interventions, on the dynamics of wild mosquito populations. Our current work extends this model by incorporating optimal control strategies to identify cost-effective and biologically feasible approaches to mosquito population suppression [19].

The model aggregates the aquatic stages (eggs, larvae, and pupae) into a single compartment denoted by A, simplifying the representation of the aquatic mosquito population. The adult mosquito population is structured into the following compartments: M for wild males, F for pre-oviposition females, F_s for females that have mated with wild males, M_i for *Wolbachia*-infected males, and F_{st} for females that have mated with these *Wolbachia*-infected males. This compartmental design enables a detailed and biologically relevant description of reproductive dynamics under control interventions. The interactions among these compartments are captured by the system of equations presented in (2.1). The model uses probabilistic terms to reflect mating competition. Specifically, $\frac{M}{M + M_i + F}$ represents the fraction of the total encounter potential attributed to wild males and thus denotes the probability of a young female mating with a wild male. Correspondingly, $\frac{M_i}{M + M_i + F}$ gives the fraction attributed to *Wolbachia*-infected males, which is the probability of mating with an infected male. The remaining fraction $\frac{F}{M + M_i + F}$ represents encounters that do not lead to mating. Thus, the three fractions sum to unity, representing a complete probabilistic description of mating outcomes: Successful mating with either wild or infected males, or an unsuccessful encounter. In this formulation, only young females F are included in the denominator because they constitute the sole class that is actively seeking for and receptive to a mate in our model. The mated females, F_s and F_{st}, are already paired and no longer participate in sexual competition. Accordingly, the terms $\frac{\beta MF}{M + M_i + F}$ and $\frac{\beta M_i F}{M + M_i + F}$ quantify the mating events with wild and *Wolbachia*-infected males, respectively [25, 26]. Tables 1 and 2 provide a

detailed description of the model's variables and parameters, including their biological interpretations and quasi-dimensional units.

Table 1. Types of state variables and their quasi-dimensional units, which can be either a for aquatic life stage and f for adult mosquitoes or terrestrial forms of the mosquito.

Type of variable	Description	Quasi-dimension
A	Aquatic stages of the mosquito and pupae	a
M	Wild male mosquitoes	f
F	Young females not yet laying eggs	f
F_s	Fertilized and egg-laying females	f
F_{st}	Females that have mated with *Wolbachia*-infected males	f
M_i	*Wolbachia*-infected male mosquitoes	f

Table 2. Parameters of Model (2.1), their description, and the corresponding quasi-dimension.

Symbol	Description	Quasi-dimension
ν_A	Rate of transition from aquatic to adult	$Time^{-1}$
μ_A	Natural death rate in the aquatic state	$Time^{-1}$
K	Maximum number of aquatic mosquitoes that the medium supports	Aquatic mosquitoes
μ_M	Death rate of wild malse	$Time^{-1}$
β	Natural mating rate of females by a male	$Time^{-1}$
μ_F	Death rate of young females not yet laying eggs	$Time^{-1}$
μ_{F_s}	Death rate of fertilized and egg-laying females	$Time^{-1}$
μ_{st}	Death rate of *Wolbachia*-infected females	$Time^{-1}$
μ_i	Death rate of *Wolbachia*-infected males	$Time^{-1}$
ϕ	The average amount of eggs laid per fertilized female	$Time^{-1}$
r	Sex ratio	$--$
ρ	Bio-transition factor of oviposition per reproducing vector	af^{-1}
Λ	Quantity of *Wolbachia*-infected male mosquitoes released	f
λ	Bio-transition factor to measure the successful transition from the aquatic to the adult stage	fa^{-1}

The complete system is described by the following system of ODEs:

$$\begin{cases} \dot{A}(t) = \rho\phi\left(1 - \dfrac{A(t)}{K}\right)F_s(t) - (\nu_A + \mu_A)\,A(t), \\ \dot{M}(t) = (1-r)\lambda\nu_A A(t) - \mu_M M(t), \\ \dot{F}(t) = r\lambda\nu_A A(t) - (\beta + \mu_F)F(t), \\ \dot{F}_s(t) = \dfrac{\beta M(t)}{M(t) + M_i(t) + F(t)}F(t) - \mu_{F_s}F_s(t), \\ \dot{F}_{st}(t) = \dfrac{\beta M_i(t)}{M(t) + M_i(t) + F(t)}F(t) - \mu_{st}F_{st}(t), \\ \dot{M}_i(t) = \Lambda - \mu_i M_i(t). \end{cases} \tag{2.1}$$

Since $F_{st}(t)$ does not affect any of the other compartments, the system can be reduced to the following five-dimensional system:

$$\begin{cases} \dot{A}(t) = \rho\phi\left(1 - \dfrac{A(t)}{K}\right)F_s(t) - (\nu_A + \mu_A)A(t), \\ \dot{M}(t) = (1-r)\lambda\nu_A A(t) - \mu_M M(t), \\ \dot{F}(t) = r\lambda\nu_A A(t) - (\beta + \mu_F)F(t), \\ \dot{F}_s(t) = \dfrac{\beta M(t)}{M(t) + M_i(t) + F(t)}F(t) - \mu_{F_s}F_s(t), \\ \dot{M}_i(t) = \Lambda - \mu_i M_i(t), \end{cases} \tag{2.2}$$

with the following initial conditions:

$$A(0) \geq 0, \quad M(0) \geq 0, \quad F(0) \geq 0, \quad F_s(0) \geq 0, \quad M_i(0) \geq 0.$$

Let $X(t) = (A(t),\ M(t),\ F(t),\ F_s(t),\ M_i(t))$. We have the following result.

Proposition 2.1. *The set*

$$\Omega = \left\{X \in \mathbb{R}^5_+ : A \leq K,\ M \leq \frac{(1-r)\lambda\nu_A K}{\mu_M},\ F \leq \frac{r\lambda\nu_A K}{\beta + \mu_F}, F_s \leq \frac{r\lambda\nu_A \beta K}{\mu_{F_s}(\beta + \mu_F)}, M_i \leq \frac{\Lambda}{\mu_i}\right\}$$

is positively invariant for system (2.2).

Proof. The proof of this proposition is carried out in two steps: We first show that the solutions remain positive, and second that they are bounded. For more details, see [24]. □

To characterize the dynamics of the system, we define the basic offspring number $\mathcal{N}$ as follows:

$$\mathcal{N} = \frac{(1-r)r\lambda\nu_A\beta\rho\phi}{\mu_{F_s}(\nu_A+\mu_A)[(1-r)(\beta+\mu_F)+r\mu_M]}.$$

System (2.2) always admits a trivial equilibrium:

$$E_1 = \left(0, 0, 0, 0, \frac{\Lambda}{\mu_i}\right).$$

When $\mathcal{N} > 1$, a non-trivial equilibrium $E_2 = (A^{**}, M^{**}, F^{**}, F_s^{**}, M_i^*)$ may exist, with the following components:

$$\begin{cases} A^{**} = \dfrac{\mu_M M^{**}}{(1-r)\lambda\nu_A}, \\ F^{**} = \dfrac{r\mu_M M^{**}}{(1-r)(\beta+\mu_F)}, \\ F_s^{**} = \dfrac{r\mu_M\beta(M^{**})^2}{\mu_{F_s}\left[(1-r)(\beta+\mu_F)+r\mu_M\right]M^{**} + (1-r)(\beta+\mu_F)M_i^*} \\ M_i^* = \dfrac{\Lambda}{\mu_i}. \end{cases}$$

The equilibrium value M^{**} is given as a root of the quadratic equation:

$$g(M^{**}) = a_1(M^{**})^2 + a_2M^{**} + a_3 = 0, \tag{2.3}$$

where the coefficients are given by:

$$\begin{aligned} a_1 &= \frac{r\mu_M\beta\rho\phi}{\mu_{F_s}K(\nu_A+\mu_A)\left[(1-r)(\beta+\mu_F)+r\mu_M\right]}, \\ a_2 &= 1-\mathcal{N}, \\ a_3 &= \frac{(1-r)(\beta+\mu_F)M_i^*}{(1-r)(\beta+\mu_F)+r\mu_M}. \end{aligned}$$

As demonstrated in [24], when $\mathcal{N} > 1$ and the density of released *Wolbachia*-infected males satisfies $M_i^* < M_i^{\text{crit}}$, with

$$M_i^{\text{crit}} = \frac{r\lambda^2\nu_A^2\beta\rho\phi K(1-r)\left(1-\dfrac{1}{\mathcal{N}}\right)^2}{4\mu_M\mu_{F_s}(\nu_A+\mu_A)(\beta+\mu_F)},$$

System (2.2) admits two positive endemic equilibria E_2^- and E_2^+. The equilibrium points E_2^- and E_2^+ are given by

$$E_2^{\pm} = \left(A_{\pm}^{**}, M_{\pm}^{**}, F_{\pm}^{**}, F_{s\pm}^{**}, M_i^*\right),$$

where

$$\begin{cases} A_{\pm}^{**} = \dfrac{\mu_M M_{\pm}^{**}}{(1-r)\,\lambda \nu_A}, \\ M_{\pm}^{**} = \dfrac{\nu_A \theta K (1-r)\lambda}{2\mu_M \mathcal{N}} \left((\mathcal{N}-1) \pm \sqrt{\dfrac{4\mu_M \mu_{F_s} (\nu_A + \omega + \mu_A)(\beta + \mu_F)\mathcal{N}^2 \left(M_i^{crit} - M_i^*\right)}{r\lambda^2 \nu_A^2 \beta \rho \phi \theta K (1-r)}} \right), \\ F_{\pm}^{**} = \dfrac{r\mu_M M_{\pm}^{**}}{(1-r)(\beta+\mu_F)}, \\ F_{s\pm}^{**} = \dfrac{r\mu_M \beta \left(M_{\pm}^{**}\right)^2}{\mu_{F_s}\left[\left((1-r)(\beta+\mu_F) + r\mu_M\right) M_{\pm}^{**} + (1-r)(\beta+\mu_F) M_i^*\right]}. \end{cases}$$

Theorem 2.1. *The qualitative behavior of the equilibria is characterized as follows:*

(i) The trivial equilibrium E_1 is globally asymptotically stable if $\mathcal{N} \leq 1$ and unstable if $\mathcal{N} > 1$ and $M_i^* < M_i^{crit}$.

(ii) If $\mathcal{N} > 1$ and $M_i^* < M_i^{crit}$, then the equilibrium E_2^- is unstable, while E_2^+ is locally asymptotically stable.

(iii) If $\mathcal{N} > 1$ and $M_i^* > M_i^{crit}$, then the trivial equilibrium E_1 is globally asymptotically stable.

Proof. The proof of these results, detailed in [24], relies on a Lyapunov stability analysis. Briefly, the stability of the trivial equilibrium E_1 is established by constructing a suitable Lyapunov function and applying LaSalle's invariance principle. The condition $\mathcal{N} \leq 1$ ensures that the derivative of the Lyapunov function along the system's trajectories is negative semi-definite, leading to the global asymptotic stability of E_1. For $\mathcal{N} > 1$, the instability of E_1 and the local stability of E_2^+ are demonstrated via linear analysis (eigenvalues of the Jacobian). □

3. The optimal control problem

Vector control remains a cornerstone in mitigating the spread of mosquitoe-borne diseases, and designing efficient intervention strategies is important for public health management. In this study, we aim to develop an optimal control framework that minimizes the overall cost associated with managing the mosquito population, while ensuring effective suppression of the vector responsible for disease transmission.

We consider two time-dependent control strategies:

- $u_1(t) \geq 0$: The investment in larvicide treatment at time t, aimed at reducing the survival of mosquito larvae in the aquatic stage;
- $u_2(t) \geq 0$: The investment in the release of *Wolbachia*-infected male mosquitoes at time t, intended to disrupt the reproductive cycle.

The control variable $u_1(t)$ influences the mortality rate in the aquatic compartment $A(t)$, effectively curbing the development of larvae into adult mosquitoes. The control $u_2(t)$ contributes directly to the growth of the *Wolbachia*-infected male population $M_i(t)$, thereby increasing the probability that wild females mate with *Wolbachia*-infected males. These unsuccessful mating events prevent fertilization, ultimately reducing the number of viable offspring.

The principal biological target of the control is the population of fertilized female mosquitoes $F_s(t)$, as they are solely responsible for egg-laying and thus the perpetuation of the mosquito life cycle and potential disease transmission. By reducing this compartment, we aim to impair the reproductive capacity of the population and prevent future outbreaks.

To mathematically capture this objective, we define a cost functional $J(u_1, u_2)$ that accounts for both the epidemiological and economic aspects of the intervention:

$$J(u_1, u_2) = F_s(T) + \int_0^T \left[c_1 F_s(t) + \frac{1}{2} \left(c_2 u_1^2(t) + c_3 u_2^2(t) \right) \right] dt, \tag{3.1}$$

where:

- $F_s(T)$ is the number of fertilized female mosquitoes at the final time T, reflecting the long-term impact of the intervention;
- $c_1 > 0$ represents the social cost associated with the presence of fertilized females during the intervention period;
- $c_2 > 0$ is the cost per unit of larvicide effort;
- $c_3 > 0$ is the cost per unit associated with the production and release of *Wolbachia*-infected males.

The structure of this cost functional balances public health outcomes with financial constraints. The terminal cost $F_s(T)$ penalizes ineffective strategies that allow reproductive females to persist by the end of the campaign. The integral term captures the cumulative burden of both the mosquito population and the control efforts over the entire time horizon. Notably, the quadratic forms $u_1^2(t)$ and $u_2^2(t)$ express the concept of increasing marginal costs, reflecting diminishing returns on excessive intervention intensity, which is an important consideration in resource-constrained settings.

The optimal control problem is therefore defined as the task of identifying measurable control functions $u_1^*(t)$ and $u_2^*(t)$ over the time interval $[0, T]$ such that the cost functional $J(u_1, u_2)$ is minimized. These optimal controls must satisfy the following:

- The system of nonlinear differential equations governing the mosquito population dynamics;
- The initial conditions of the system;
- The admissibility constraints $u_1(t), u_2(t) \geq 0$ for all $t \in [0, T]$.

To incorporate the control strategies into the mosquito population dynamics, we reformulate the system of differential equations by introducing the control variables $u_1(t)$ and $u_2(t)$. These controls represent, respectively, the application of larvicides and the release of *Wolbachia*-infected male mosquitoes, both of which are functions of time. The controlled system is given by:

$$\begin{cases} \dot{A}(t) = \rho\phi \left(1 - \dfrac{A(t)}{K}\right) F_s(t) - (\nu_A + \mu_A + u_1(t))\, A(t), \\ \dot{M}(t) = (1 - r)\lambda\nu_A A(t) - \mu_M M(t), \\ \dot{F}(t) = r\lambda\nu_A A(t) - (\beta + \mu_F)\, F(t), \\ \dot{F}_s(t) = \dfrac{\beta M(t)}{M(t) + M_i(t) + F(t)} F(t) - \mu_{F_s} F_s(t), \\ \dot{M}_i(t) = u_2(t) - \mu_i M_i(t), \end{cases} \tag{3.2}$$

where all variables and parameters retain their previous biological meanings, and $u_1(t)$ and $u_2(t)$ are non-negative measurable functions bounded above by $u_{1,\max}$ and $u_{2,\max}$, respectively. This system is subject to the following initial conditions, corresponding to the coordinates of a biologically relevant non-trivial equilibrium point of the uncontrolled system (i.e., when $\Lambda = 0$ in the original formulation):

$$\begin{aligned} A(0) &= A_0 = \frac{\mu_M M_0}{(1-r)\lambda v_A}, \\ M(0) &= M_0 = \frac{\lambda v_A K(1-r)(\mathcal{N}-1)}{\mu_M \mathcal{N}}, \\ M_i(0) &= M_{i0} = 0, \\ F(0) &= F_0 = \frac{r\mu_M M_0}{(1-r)(\beta+\mu_F)}, \\ F_s(0) &= F_{s0} = \frac{r\mu_M \beta M_0}{\mu_{F_s}\left[(1-r)(\beta+\mu_F)+r\mu_M\right]}. \end{aligned}$$

These initial values represent a stable, endemic configuration of the mosquito population before the application of any control interventions, providing a realistic starting point for evaluating the effects of control policies [18].

The objective remains to determine an optimal control pair $(u_1^*(t), u_2^*(t))$ that minimizes the total cost functional $J(u_1, u_2)$, as defined in (3.1), over a fixed time horizon $[0, T]$. This is formalized as the following optimization problem:

$$J(u_1^*, u_2^*) = \min\{J(u_1, u_2) \mid (u_1, u_2) \in \Gamma\}, \tag{3.3}$$

where the admissible control set Γ is defined by:

$$\Gamma = \{(u_1, u_2) \,\big|\, 0 \le u_i(t) \le u_{i,\max},\ i = 1, 2\}. \tag{3.4}$$

3.1. Existence of an optimal control

We now establish the existence of an optimal control for the system under consideration, based on the classical theory of optimal control.

Theorem 3.1. *There is an optimal control pair* $(u_1^*, u_2^*) \in \Gamma$ *such that*

$$J(u_1^*, u_2^*) = \min_{(u_1,u_2)\in\Gamma} J(u_1, u_2).$$

Proof. The proof is organized in four steps.

Step 1: Boundedness of trajectories.
According to Proposition 2.1, the state variables A, M, F, F_s, and M_i are positive and bounded. Thus, a compact set $\mathcal{K} \subset \mathbb{R}^5_+$ exists such that $X(t) \in \mathcal{K}$ for all $t \in [0, T]$ and all admissible controls, with

$$\mathcal{K} = \left\{X \in \mathbb{R}^5_+ : A \le K,\ M \le \frac{(1-r)\lambda v_A K}{\mu_M},\ F \le \frac{r\lambda v_A K}{\beta+\mu_F}, F_s \le \frac{r\lambda v_A \beta K}{\mu_{F_s}(\beta+\mu_F)}, M_i \le \frac{u_{2,\max}}{\mu_i}\right\}.$$

Step 2: We show that if $M(0) > 0$ and $F(0) > 0$, then $M(t) > 0$ and $F(t) > 0$ for all t. Indeed, from

$$\dot{M}(t) = (1 - r)\lambda\nu_A A(t) - \mu_M M(t) \geq -\mu_M M(t),$$

we obtain $M(t) \geq M(0)e^{-\mu_M t} > 0$. Similarly,

$$\dot{F}(t) = r\lambda\nu_A A(t) - (\beta + \mu_F)F(t) \geq -(\beta + \mu_F)F(t) \Rightarrow F(t) \geq F(0)e^{-(\beta+\mu_F)t} > 0.$$

Since $M_i(t) \geq 0$, we have $M(t) + M_i(t) + F(t) \geq M(t) + F(t) > 0$ for all t. Therefore, the function $\frac{MF}{M+M_i+F}$ is Lipschitz continuous on the trajectory, because the denominator is bounded away from zero.

Step 3: Existence and uniqueness of solutions for measurable controls.
The right-hand side of System (3.2) is measurable in t (since u_1, u_2 are measurable) and, on the compact set $\mathcal{K}$ containing the trajectory, it is Lipschitz in X. By Carathéodory's existence theorem for ODEs with measurable time dependence [27], there is a unique absolutely continuous solution $X(t)$ defined on $[0, T]$ for each admissible control pair.

Step 4: Verification of the Filippov–Cesari conditions [28].

(i) For each admissible control pair $(u_1, u_2) \in \Gamma$, the corresponding state system (3.2) admits a unique solution

$$X(t) = (A(t), M(t), F(t), F_s(t), M_i(t))$$

defined on the interval $[0, T]$. Furthermore, the state variables remain bounded on $[0, T]$ for all admissible controls(Steps 1 and 3).

(ii) The sets of admissible initial conditions $X(0)$ and final states $X(T)$ lie in a compact subset of $\mathbb{R}^5_+$.

(iii) The control set Γ consists of Lebesgue measurable functions $u_1(t)$ and $u_2(t)$ such that $0 \leq u_1(t) \leq u_{1,\max}$ and $0 \leq u_2(t) \leq u_{2,\max}$ for all $t \in [0, T]$. This set is convex, closed, and bounded in the $L^2([0, T])$ norm.

(iv) The right-hand side of the system (3.2) is continuously differentiable with respect to the state variables and affine (hence Lipschitz) in the control variables u_1 and u_2 (Step 2).

(v) The cost functional $J(u_1, u_2)$, including any terminal terms, is continuous with respect to the state and control variables.

(vi) The integrand of the objective functional is strictly convex in (u_1, u_2) and satisfies a coercivity condition of the form

$$c_1 F_s(t) + \frac{1}{2}\left(c_2 u_1^2(t) + c_3 u_2^2(t)\right) \geq \delta_1 \left(\|u_1\|^2 + \|u_2\|^2\right)^{\alpha/2} - \delta_2,$$

for some constants $\delta_1 > 0$, $\alpha > 1$, and $\delta_2 \geq 0$. In our case, this condition holds with $\delta_1 = \min\left\{\frac{c_2}{2}, \frac{c_3}{2}\right\}$, $\alpha = 2$, and $\delta_2 = 0$.

Since all the conditions above are satisfied, the existence result stated in Theorem 4.1 of [28] ensures the existence of an optimal control pair $(u_1^*, u_2^*) \in \Gamma$ minimizing the cost functional over all admissible controls.

□

3.2. Characterization of the optimal control problem

We apply the Pontryagin maximum principle [28, 29] to derive the characterization of the optimal control pair (u_1^*, u_2^*). Let the state vector be $X = (A, M, F, F_s, M_i)$, the control vector be $U = (u_1, u_2)$, and the adjoint vector be $Z = (\lambda_1, \lambda_2, \lambda_3, \lambda_4, \lambda_5)$. The Hamiltonian associated with the system is defined as:

$$\begin{aligned} H(X,U,Z) = {} & c_1 F_s(t) + \frac{1}{2}c_2 u_1^2(t) + \frac{1}{2}c_3 u_2^2(t) \\ & + \lambda_1 \left[\rho\phi\left(1 - \frac{A(t)}{K}\right)F_s(t) - (\nu_A + \mu_A + u_1(t))A(t)\right] \\ & + \lambda_2 \left[(1-r)\lambda\nu_A A(t) - \mu_M M(t)\right] \\ & + \lambda_3 \left[r\lambda\nu_A A(t) - (\beta + \mu_F)F(t)\right] \\ & + \lambda_4 \left[\frac{\beta M(t)}{M(t) + M_i(t) + F(t)}F(t) - \mu_{F_s}F_s(t)\right] \\ & + \lambda_5 \left[u_2(t) - \mu_i M_i(t)\right], \end{aligned}$$

where $\lambda_i(t)$, $i = 1, \ldots, 5$, are the adjoint variables corresponding to the state components.

Let $U^* = (u_1^*, u_2^*)$ denote the optimal control pair associated with the optimal state trajectory $X^*(t) = (A^*(t), M^*(t), F^*(t), F_s^*(t), M_i^*(t))$, defined over the time interval $[0, T]$.

The adjoint system is given by:

$$\begin{aligned} \dot{\lambda}_1(t) &= -\frac{\partial H}{\partial A} = \left(\rho\phi\frac{F_s^*(t)}{K} + \nu_A + \mu_A + u_1^*(t)\right)\lambda_1 \\ &\quad - (1-r)\lambda\nu_A\lambda_2 - r\lambda\nu_A\lambda_3, \\ \dot{\lambda}_2(t) &= -\frac{\partial H}{\partial M} = \mu_M\lambda_2 - \frac{\beta(M_i^*(t) + F^*(t))F^*(t)}{(M^*(t) + M_i^*(t) + F^*(t))^2}\lambda_4, \\ \dot{\lambda}_3(t) &= -\frac{\partial H}{\partial F} = (\beta + \mu_F)\lambda_3 - \frac{\beta(M^*(t) + M_i^*(t))M^*(t)}{(M^*(t) + M_i^*(t) + F^*(t))^2}\lambda_4, \\ \dot{\lambda}_4(t) &= -\frac{\partial H}{\partial F_s} = -c_1 - \rho\phi\left(1 - \frac{A^*(t)}{K}\right)\lambda_1 + \mu_{F_s}\lambda_4, \\ \dot{\lambda}_5(t) &= -\frac{\partial H}{\partial M_i} = \frac{\beta M^*(t)F^*(t)}{(M^*(t) + M_i^*(t) + F^*(t))^2}\lambda_4 + \mu_i\lambda_5. \end{aligned}$$

The associated transversality conditions at the terminal time T are

$$\lambda_1(T) = \lambda_2(T) = \lambda_3(T) = 0, \quad \lambda_4(T) = -\frac{\partial Fs(T)}{\partial X}\bigg|_{X=X(T)} = 1, \quad \lambda_5(T) = 0.$$

From [30], the second order conditions for optimality hold, as follows:

$$\frac{\partial^2 H}{\partial u_1^2} = c_2 > 0, \quad \frac{\partial^2 H}{\partial u_2^2} = c_3 > 0,$$

which guarantees that the Hamiltonian is minimized at $U^*(t)$. Therefore,

$$H(X^*(t), U^*(t), Z(t)) \leq H(X^*(t), U(t), Z(t)) \quad \forall\, U \in \Gamma,\ \forall\, t \in [0, T]. \tag{3.5}$$

The characterization of the optimal controls follows from:

$$\begin{cases} \dfrac{\partial H}{\partial u_1}(X^*, U^*, Z) = c_2 u_1^*(t) - \lambda_1(t) A^*(t) = 0, \\ \dfrac{\partial H}{\partial u_2}(X^*, U^*, Z) = c_3 u_2^*(t) + \lambda_5(t) = 0. \end{cases} \tag{3.6}$$

Considering the control bounds, the optimal controls satisfy the projection formula [30]:

$$\begin{cases} u_i^*(t) = 0 & \text{if } \dfrac{\partial H}{\partial u_i} > 0, \\ 0 < u_i^*(t) < u_{i,\max} & \text{if } \dfrac{\partial H}{\partial u_i} = 0, \qquad i = 1, 2. \\ u_i^*(t) = u_{i,\max} & \text{if } \dfrac{\partial H}{\partial u_i} < 0, \end{cases} \tag{3.7}$$

Therefore, the expressions for the optimal controls are:

$$u_1^*(t) = \max\left\{0, \min\left\{\frac{A^*(t)}{c_2}\lambda_1(t),\ u_{1,\max}\right\}\right\}, \tag{3.8}$$

$$u_2^*(t) = \max\left\{0, \min\left\{-\frac{1}{c_3}\lambda_5(t),\ u_{2,\max}\right\}\right\}. \tag{3.9}$$

4. Derivation of the impulsive control model

To better capture the discrete nature of interventions typically implemented in vector control programs, we develop a model incorporating impulsive control strategies. In contrast to optimal control frameworks based on continuous intervention, this approach accounts for the discrete nature of field operations such as periodic larvicide applications and mass releases of *Wolbachia*-infected male mosquitoes.

In this new framework, we explicitly introduce the larvicide concentration, denoted by $L(t)$, as a dynamic state variable [20]. This addition enhances the biological realism of the model by representing both the immediate impact of larvicidal treatments and their gradual environmental degradation. Specifically, larvicides applied at impulsive moments are assumed to decay exponentially over time, characterized by a degradation rate m_2. Their lethal effect on aquatic mosquito stages is modeled through a mortality rate m_1, assumed to be proportional to the larvicide concentration in the environment.

Moreover, *Wolbachia*-infected male mosquitoes, denoted by $M_i(t)$, are introduced at discrete times that are integer multiples of the release period τ_1. Between release events, their population declines according to a natural mortality rate μ_i. The number of *Wolbachia*-infected males released at each pulse is constant and denoted by Λ, while the volume of larvicide applied at each impulsive time τ_2 is denoted by l_i.

The resulting model is thus formulated as a hybrid impulsive system, combining classical differential equations to describe the system's dynamics between intervention times and discrete jump conditions to capture the impact of impulsive events. This framework enables a rigorous analysis of the effects of periodic release and larviciding strategies on the overall entomological system dynamics. The system

can be described by the following set of equations:

$$\left\{\begin{array}{l} \left.\begin{array}{l} \dot{A}(t) = \rho\phi\left(1-\dfrac{A(t)}{K}\right)F_s(t) - (\nu_A+\mu_A)A(t) - m_1L(t)A(t), \\ \dot{M}(t) = (1-r)\lambda\nu_A A(t) - \mu_M M(t), \\ \dot{F}(t) = r\lambda\nu_A A(t) - (\beta+\mu_F)F(t), \\ \dot{F}_s(t) = \dfrac{\beta M(t)}{M(t)+M_i(t)+F(t)}F(t) - \mu_{F_s}F_s(t), \\ \dot{M}_i(t) = -\mu_i M_i(t), \\ \dot{L}(t) = -m_2L(t), \end{array}\right\} \quad t \neq n\tau_1,\ n\tau_2 \\ \left.\begin{array}{ll} M_i(t^+) = M_i(t^-) + \Lambda, & \text{at } t = n\tau_1, \\ L(t^+) = L(t^-) + l_i, & \text{at } t = n\tau_2, \end{array}\right\} \quad \text{with} \quad n = 1,2,3,\ldots. \end{array}\right. \tag{4.1}$$

The notations $M_i(t^-)$, $L(t^-)$, $M_i(t^+)$, and $L(t^+)$ denote the values of the corresponding variables immediately before and after the impulsive interventions.

The main advantage of this formulation is twofold. On the one hand, it enables the identification of asymptotic periodic solutions of the impulsive system (4.1), which correspond to stationary regimes under impulsive interventions. On the other hand, it facilitates the determination of critical thresholds for the quantity of interventions (i.e., Λ^*, l_i^*) that ensure either the successful invasion of the wild population by infected mosquitoes or, conversely, its elimination.

By adopting this impulsive framework, our model closely mirrors the operational practices of vector control campaigns conducted in the field, while also providing robust mathematical tools for strategy optimization. This level of modeling is particularly well-suited to the realities of tropical settings, where resources are limited and interventions must be discrete, targeted, and economically justified.

We now turn to the mathematical analysis of System (4.1). Let the state vector be defined as $X(t) = (A(t), M(t), F(t), F_s(t), M_i(t), L(t))$. Following the approach in [20, 23], we analyze the dynamics of the impulsive subsystems governing the release of *Wolbachia*-infected males and the application of larvicides. These are given by as follows:

$$\left\{\begin{array}{ll} \dot{M}_i(t) = -\mu_i M_i(t), & t \neq n\tau_1, \\ M_i(t^+) = M_i(t) + \Lambda, & t = n\tau_1, \end{array}\right. \tag{4.2}$$

$$\left\{\begin{array}{ll} \dot{L}(t) = -m_2L(t), & t \neq n\tau_2, \\ L(t^+) = L(t) + l_i, & t = n\tau_2. \end{array}\right. \tag{4.3}$$

These impulsive systems admit a unique, positive, and periodic solution given, respectively, by

$$M_i^*(t) = \frac{\Lambda e^{-\mu_i(t-n\tau_1)}}{1-e^{-\mu_i\tau_1}}, \quad n\tau_1 < t \leq (n+1)\tau_1, \tag{4.4}$$

$$L^*(t) = \frac{l_i e^{-m_2(t-n\tau_2)}}{1-e^{-m_2\tau_2}}, \quad n\tau_2 < t \leq (n+1)\tau_2. \tag{4.5}$$

According to [23], we have the following result.

Lemma 4.1. *For any solution $M_i(t)$ of System* (4.2) *and $L(t)$ of System* (4.3)*, with the initial conditions $M_i(0^+) \geq 0$ and $L(0^+) \geq 0$, we have the following asymptotic behavior:*

$$M_i(t) \to M_i^*(t) \quad as \quad t \to \infty, \quad and \quad L(t) \to L^*(t) \quad as \quad t \to \infty.$$

Thus, $M_i(t)$ and $L(t)$ can be replaced by their periodic solutions in System (4.1) to obtain the simplified system (4.6), as shown in [24, 31]:

$$\begin{cases} \dot{A}(t) = \rho\phi\left(1 - \dfrac{A(t)}{K}\right)F_s(t) - (\nu_A + \mu_A)A(t) - m_1 L^*(t)A(t), \\ \dot{M}(t) = (1-r)\lambda\nu_A A(t) - \mu_M M(t), \\ \dot{F}(t) = r\lambda\nu_A A(t) - (\beta + \mu_F)F(t), \\ \dot{F}_s(t) = \dfrac{\beta M(t)}{M(t) + M_i^*(t) + F(t)}F(t) - \mu_{F_s}F_s(t), \end{cases} \tag{4.6}$$

with the initial conditions

$$A(0) \geq 0,\ M(0) \geq 0,\ F(0) \geq 0, \text{ and } F_s(0) \geq 0$$

Using Relations (4.4) and (4.5), we can bound the periodic solutions as follows:

$$M_{i,\min}^* \leq M_i^*(t) \leq M_{i,\max}^*, \tag{4.7}$$

where

$$M_{i,\min}^* = \frac{\Lambda e^{-\mu_i\tau_1}}{1 - e^{-\mu_i\tau_1}}, \quad M_{i,\max}^* = \frac{\Lambda}{1 - e^{-\mu_i\tau_1}},$$

and similarly for $L^*(t)$:

$$L_{\min}^* \leq L^*(t) \leq L_{\max}^*, \tag{4.8}$$

where

$$L_{\min}^* = \frac{l_i e^{-m_2\tau_2}}{1 - e^{-m_2\tau_2}}, \quad L_{\max}^* = \frac{l_i}{1 - e^{-m_2\tau_2}}.$$

4.1. Boundedness of the solutions

In this section, we establish that the solutions of system (4.1) remain bounded for all $t \geq 0$. This is an essential property to ensure the mathematical well-posedness of the model and to confirm that it yields biologically realistic predictions over time.

Theorem 4.1. *Let $(A(t), M(t), F(t), F_s(t), M_i(t), L(t))$ be any solution of system* (4.1) *with non-negative initial conditions. Then, all state variables remain non-negative for all $t \geq 0$ and a positive constant $\delta > 0$ exists such that, for all $t \geq 0$, the following inequalities hold:*

$$A(t) \leq \delta, \quad M(t) \leq \delta, \quad F(t) \leq \delta, \quad F_s(t) \leq \delta, \quad M_i(t) \leq \delta, \quad L(t) \leq \delta.$$

Proof. The proof is organized into five steps.

Step 1: Positivity of all state variables.

Let $(A(t), M(t), F(t), F_s(t), M_i(t), L(t))$ be a solution of system (4.1) with non-negative initial conditions.

For $t \neq n\tau_1, n\tau_2$, the system is governed by ODEs with locally Lipschitz continuous right-hand sides. Using standard comparison arguments [24, 29], we obtain:

$$A(t) \geq 0, \quad M(t) \geq 0, \quad F(t) \geq 0, \quad F_s(t) \geq 0,$$

for all $t \geq 0$, provided that the initial conditions are non-negative.

Indeed, from the first equation of (4.1), we have

$$\dot{A}(t) \geq -(\nu_A + \mu_A + m_1 L^*(t))A(t),$$

which implies

$$A(t) \geq A(0) \exp\left(-\int_0^t (\nu_A + \mu_A + m_1 L^*(s))ds\right) > 0,$$

whenever $A(0) > 0$. Similar arguments apply to $M(t)$, $F(t)$, and $F_s(t)$.

Moreover, the impulsive conditions satisfy:

$$M_i(t^+) = M_i(t^-) + \Lambda \geq 0,$$

and

$$L(t^+) = L(t^-) + l_i \geq 0.$$

Consequently, all state variables remain non-negative for all $t \geq 0$.

Step 2: Boundedness of A, M, F and F_s.

Between impulsive instants, the dynamics of A, M, F, and F_s are governed by the same equations as in system (2.1), since the impulsive controls act directly only on M_i and L. Moreover, these variables remain continuous at impulsive times, as the jumps affect only M_i and L. Consequently, the bounds established in Proposition 2.1 hold for all $t \geq 0$. We thus obtain the following inequalities:

$$A(t) \leq \kappa_A = K, \quad M(t) \leq \kappa_M = \frac{(1-r)\lambda\nu_A K}{\mu_M},$$

$$F(t) \leq \kappa_F = \frac{r\lambda\nu_A K}{\beta + \mu_F}, \quad F_s(t) \leq \kappa_{F_s} = \frac{r\lambda\nu_A \beta K}{\mu_{F_s}(\beta + \mu_F)}.$$

These bounds hold for every $t \geq 0$, including at the impulsive times.

Step 3: Uniform boundedness of $M_i(t)$.

For $t \neq n\tau_1$, the dynamics of M_i are given by $\dot{M}_i = -\mu_i M_i$. On each interval $(n\tau_1, (n+1)\tau_1]$, we have:

$$M_i(t) = M_i(n\tau_1^+)e^{-\mu_i(t-n\tau_1)} \leq M_i(n\tau_1^+),$$

since the exponential factor is less than or equal to 1. It therefore suffices to bound M_i at the impulsive times.

At each impulsive instant $t = n\tau_1$, the variable M_i undergoes the following jump:

$$M_i(n\tau_1^+) = M_i(n\tau_1^-) + \Lambda.$$

Iterating from $t = 0^+$, we obtain:

$$M_i(n\tau_1^+) = M_i(0^+)e^{-\mu_i n\tau_1} + \Lambda \sum_{k=0}^{n-1} e^{-\mu_i k\tau_1}.$$

The sum is a geometric series. Since $\mu_i > 0$ and $\tau_1 > 0$, we have $e^{-\mu_i\tau_1} < 1$, and therefore:

$$\sum_{k=0}^{n-1} e^{-\mu_i k\tau_1} \leq \sum_{k=0}^{\infty} e^{-\mu_i k\tau_1} = \frac{1}{1 - e^{-\mu_i\tau_1}}.$$

Moreover, $e^{-\mu_i n\tau_1} \leq 1$ for all $n \geq 0$. Hence:

$$M_i(n\tau_1^+) \leq M_i(0^+) + \frac{\Lambda}{1 - e^{-\mu_i\tau_1}}.$$

The right-hand side is independent of n. Consequently, for any $t \geq 0$, we obtain:

$$M_i(t) \leq M_i(n\tau_1^+) \leq M_i(0^+) + \frac{\Lambda}{1 - e^{-\mu_i\tau_1}} = \kappa_{M_i}.$$

Thus, M_i is uniformly bounded by a constant independent of t and n.

Step 4: Uniform boundedness of $L(t)$.
An analogous argument applies to $L(t)$. For $t \neq n\tau_2$, we have $\dot{L} = -m_2 L$, and at each impulsive instant $t = n\tau_2$, $L(n\tau_2^+) = L(n\tau_2^-) + l_i$. Repeating the argument yields:

$$L(t) \leq L(0^+) + \frac{l_i}{1 - e^{-m_2\tau_2}} = \kappa_L \quad \text{for all } t \geq 0.$$

Step 5: Final uniform bound.
Define the constant:

$$\delta = \max\left\{\kappa_A,\ \kappa_M,\ \kappa_F,\ \kappa_{F_s},\ \kappa_{M_i},\ \kappa_L\right\}.$$

Then, by construction, for all $t \geq 0$, we have

$$A(t) \leq \delta, \quad M(t) \leq \delta, \quad F(t) \leq \delta, \quad F_s(t) \leq \delta, \quad M_i(t) \leq \delta, \quad L(t) \leq \delta.$$

The constant δ depends only on the model parameters and the initial conditions, not on time nor on the pulse indices. This completes the proof.

□

4.2. Existence and stability of periodic solutions

In this section, we analyze the existence and stability of periodic solutions of System (4.1), with a particular focus on both trivial and non-trivial periodic solutions.

4.2.1. Existence and local stability of a trivial periodic solution

We begin by examining the existence of a trivial periodic solution. This situation corresponds to the absence of wild mosquitoes in the environment, i.e., $A(t) = 0$, $M(t) = 0$, $F(t) = 0$, and $F_s(t) = 0$ for all t. Thus, System (4.1) admits a trivial periodic solution given by:

$$\mathcal{E}_{per}(t) = (A^*(t), M^*(t), F^*(t), F_s^*(t), M_i^*(t), L^*(t)) = (0, 0, 0, 0, M_i^*(t), L^*(t)),$$

where $M_i^*(t)$ and $L^*(t)$ represent the periodic dynamics of the infected male mosquitoes and larvicide concentration, respectively, maintained through periodic impulsive releases; these are explicitly defined in Eqs (4.4) and (4.5).

Theorem 4.2. *The trivial periodic solution* $\mathcal{E}_{per}(t) = \left(0, 0, 0, 0, M_i^*(t), L^*(t)\right)$ *of system* (4.1) *is locally asymptotically stable.*

Proof. To analyze the local stability of the periodic solution $\mathcal{E}_{per}(t)$, we introduce small perturbations around the mosquito-free equilibrium point [32–34]. We establish the local stability of the trivial periodic solution for $t = n\tau_1 = n\tau_2 = n\tau$ and for $\tau_1 \neq \tau_2$. Let

$$\begin{cases} x(t) = A(t) - A^*(t), \\ y(t) = M(t) - M^*(t), \\ z(t) = F(t) - F^*(t), \\ s(t) = F_s(t) - F_s^*(t), \\ v(t) = M_i(t) - M_i^*(t), \\ w(t) = L(t) - L^*(t), \end{cases} \tag{4.9}$$

where $x(t), y(t), z(t), s(t), v(t)$, and $w(t)$ denote the deviations of the state variables from their values at the trivial equilibrium. Shifting the periodic solution $\mathcal{E}_{per}(t)$ to the origin using the change of variables defined in system (4.9) yields the following variational system:

$$\begin{cases} \dot{x}(t) = \rho\phi\left(1 - \dfrac{x(t)}{K}\right) s(t) - (\nu_A + \mu_A)\, x(t) - m_1\, (w(t) + L^*(t))\, x(t), \\ \dot{y}(t) = (1 - r)\lambda\nu_A x(t) - \mu_M y(t), \\ \dot{z}(t) = r\lambda\nu_A x(t) - (\beta + \mu_F) z(t), \\ \dot{s}(t) = \dfrac{\beta y(t)}{y(t) + v(t) + M_i^*(t) + z(t)} z(t) - \mu_{F_s} s(t), \\ \dot{v}(t) = -\mu_i v(t), \\ \dot{w}(t) = -m_2 w(t), \end{cases} \qquad \text{for } t \neq n\tau_1,\ n\tau_2, \tag{4.10}$$

with the impulsive effects defined by

$$\begin{aligned} v(t^+) &= v(t), \qquad \text{at } t = n\tau_1, \\ w(t^+) &= w(t), \qquad \text{at } t = n\tau_2. \end{aligned}$$

System (4.10) can be expressed in matrix form as

$$\begin{pmatrix} x(t) \\ y(t) \\ z(t) \\ s(t) \\ v(t) \\ w(t) \end{pmatrix} = \Psi(t) \begin{pmatrix} x(0) \\ y(0) \\ z(0) \\ s(0) \\ v(0) \\ w(0) \end{pmatrix},$$

where the fundamental matrix solution $\Psi(t)$ satisfies

$$\frac{d\Psi(t)}{dt} = B(t)\Psi(t), \quad \Psi(0) = I,$$

where I denotes the identity matrix and the Jacobian matrix $B(t)$ given by:

$$B(t) = \begin{pmatrix} -(\frac{\rho\phi s(t)}{K}\nu_A + \mu_A + m_1 L^*(t)) & 0 & 0 & \rho\phi\left(1 - \frac{x(t)}{K}\right) & 0 & 0 \\ (1-r)\lambda\nu_A & -\mu_M & 0 & 0 & 0 & 0 \\ r\lambda\nu_A & 0 & -(\beta + \mu_F) & 0 & 0 & 0 \\ 0 & a_1 & a_2 & -\mu_{F_s} & a_3 & 0 \\ 0 & 0 & 0 & 0 & -\mu_i & 0 \\ 0 & 0 & 0 & 0 & 0 & -m_2 \end{pmatrix},$$

where

$$\begin{cases} a_1 = \dfrac{\beta z(t)\left(v(t) + M_i^*(t) + z(t)\right)}{\left(y(t) + v(t) + M_i^*(t) + z(t)\right)^2}, \\ a_2 = \dfrac{\beta y(t)\left(y(t) + v(t) + M_i^*(t)\right)}{\left(y(t) + v(t) + M_i^*(t) + z(t)\right)^2}, \\ a_3 = \dfrac{-\beta y(t) z(t)}{\left(y(t) + v(t) + M_i^*(t) + z(t)\right)^2}. \end{cases}$$

Thus, when $x(t) = 0$, $y(t) = 0$, $z(t) = 0$, and $s(t) = 0$, we obtain the following linear system:

$$\frac{d\Psi(t)}{dt} = B_0(t)\Psi(t),$$

with

$$B_0(t) = \begin{pmatrix} -(\nu_A + \mu_A + m_1 L^*(t)) & 0 & 0 & \rho\phi & 0 & 0 \\ (1-r)\lambda\nu_A & -\mu_M & 0 & 0 & 0 & 0 \\ r\lambda\nu_A & 0 & -(\beta + \mu_F) & 0 & 0 & 0 \\ 0 & 0 & 0 & -\mu_{F_s} & 0 & 0 \\ 0 & 0 & 0 & 0 & -\mu_i & 0 \\ 0 & 0 & 0 & 0 & 0 & -m_2 \end{pmatrix}.$$

From the theory of linear periodic systems and Floquet theory [35], the stability of the trivial periodic solution is determined by the characteristic multipliers θ_i, which are the eigenvalues of the monodromy

matrix $\Psi(\tau)$. If we let $\theta_1, \ldots, \theta_6$ be the characteristic multipliers, then:

$$\theta_1 = \exp\left(-\int_0^\tau (\nu_A + \mu_A + m_1 L^*(t))\, dt\right),$$
$$\theta_2 = \exp\left(-\int_0^\tau \mu_M dt\right),$$
$$\theta_3 = \exp\left(-\int_0^\tau (\beta + \mu_F) dt\right),$$
$$\theta_4 = \exp\left(-\int_0^\tau \mu_{F_s} dt\right),$$
$$\theta_5 = \exp\left(-\int_0^\tau \mu_i dt\right),$$
$$\theta_6 = \exp\left(-\int_0^\tau m_2 dt\right).$$

Since all parameters are strictly positive, it follows that $0 < \theta_i < 1$ for $i = 2, \ldots, 6$. To ensure local asymptotic stability, it suffices to show that $0 < \theta_1 < 1$. We now consider two cases.

(i) When larvicide applications and releases of *Wolbachia*-infected males occur simultaneously, (i.e., $t = n\tau_1 = n\tau_2 = n\tau$), the larvicide concentration satisfies

$$L^*(t) = \frac{l_i e^{-m_2(t-n\tau)}}{1 - e^{-m_2\tau}}.$$

Thus

$$\int_0^\tau (\nu_A + \mu_A + m_1 L^*(t))\, dt > 0 \quad \Rightarrow \quad 0 < \theta_1 < 1.$$

Hence, $\mathcal{E}_{per}(t)$ is locally asymptotically stable in this case.

(ii) If $\tau_1 \neq \tau_2$, then we distinguish the following subcases:

– At times $t = n\tau_1$, no larvicide is applied ($l_i = 0$); hence $L^*(t) = 0$, and:

$$\int_0^\tau (\nu_A + \mu_A) dt > 0 \quad \Rightarrow \quad 0 < \theta_1 < 1.$$

– At $t = n\tau_2$, the infected males are not released, and the larvicide concentration is:

$$L^*(t) = \frac{l_i e^{-m_2(t-n\tau_2)}}{1 - e^{-m_2\tau_2}} > 0,$$

so again:

$$\int_0^\tau (\nu_A + \mu_A + m_1 L^*(t)) dt > 0 \quad \Rightarrow \quad 0 < \theta_1 < 1.$$

Therefore, even in the non-synchronized case, all characteristic multipliers satisfy $0 < \theta_i < 1$, and $\mathcal{E}_{per}(t)$ remains locally asymptotically stable.

□

4.2.2. Existence of non-trivial periodic solutions

For the notion of periodicity to be well-defined, we assume that the impulsive periods satisfy

$$\frac{\tau_1}{\tau_2} \in \mathbb{Q},$$

so a common period $T = \text{lcm}(\tau_1, \tau_2) > 0$ exists such that $M_i^*(t)$ and $L^*(t)$ are both T-periodic. Without loss of generality, we shall hereafter consider the simplified case $\tau_1 = \tau_2 = \tau$, so that $T = \tau$. For the analysis of positive time-dependent solutions, we consider the following reduced algebraic system:

$$\begin{cases} \rho\phi\left(1 - \dfrac{x(t)}{K}\right) s(t) - (\nu_A + \mu_A)\, x(t) - m_1 L^*(t) x(t) = 0, \\ (1-r)\lambda\nu_A x(t) - \mu_M y(t) = 0, \\ r\lambda\nu_A x(t) - (\beta + \mu_F)\, z(t) = 0, \\ \dfrac{\beta y(t)}{y(t) + M_i^*(t) + z(t)} z(t) - \mu_{F_s} s(t) = 0, \\ v(t) = 0, \\ w(t) = 0. \end{cases} \tag{4.11}$$

Solving system (4.11) leads to the quadratic equation:

$$\frac{N^*(t)}{K} x^2(t) + (1 - N^*(t))\, x(t) + \frac{\mu_M\,(\beta + \mu_F)}{\lambda\nu_A\left[(1-r)(\beta+\mu_F) + r\mu_M\right]} M_i^*(t) = 0, \tag{4.12}$$

where

$$N^*(t) = \frac{(1-r) r\lambda\nu_A\beta\rho\phi}{\mu_{F_s}\,(\nu_A + \mu_A + m_1 L^*(t))\left[(1-r)(\beta+\mu_F) + r\mu_M\right]} \tag{4.13}$$

is the local offspring number at time t.
Setting $1 - N^*(t) = 0$, we obtain:

$$L^*(t) = \frac{\nu_A + \mu_A}{m_1}\,(\mathcal{N} - 1)\,,$$

where

$$\mathcal{N} = \frac{(1-r) r\lambda\nu_A\beta\rho\phi}{\mu_{F_s}(\nu_A + \mu_A)\left[(1-r)(\beta+\mu_F) + r\mu_M\right]}$$

is the basic offspring number defined in [24].
We define the critical larvicide concentration as:

$$L^{\text{crit}} = \frac{\nu_A + \mu_A}{m_1}\,(\mathcal{N} - 1)\,. \tag{4.14}$$

From Eq (4.12), note that:

$$\frac{N^*(t)}{K} > 0 \qquad \text{and} \qquad \frac{\mu_M\,(\beta + \mu_F)}{\lambda\nu_A\left[(1-r)(\beta+\mu_F) + r\mu_M\right]} M_i^*(t) > 0.$$

Thus, the existence of positive solutions $x(t) > 0$ depends on the value of $N^*(t)$. Inequality 4.8 indicates that $L^*(t)$ reaches a minimum value L^*_{min} and a maximum value L^*_{max}. Thus, for $\mathcal{N} > 1$, a threshold $L^{\text{crit}} > 0$ exists such that $N^*(t) \le 1$ if $L^*_{\text{min}} \ge L^{\text{crit}}$ and $N^*(t) > 1$ if $L^*_{\text{max}} < L^{\text{crit}}$. Consequently, we have:

- If $\mathcal{N} > 1$ and $L^*_{\min} > L^{\text{crit}}$, then Eq (4.12) admits no positive solution.
- If $\mathcal{N} > 1$ and $L^*_{\max} < L^{\text{crit}}$, then Eq (4.12) may admit 0, 1, or 2 positive solutions.

Assuming $\mathcal{N} > 1$ and $L^*_{\max} < L^{\text{crit}}$, the number of positive roots of Eq (4.12) depends on the discriminant:

$$\Delta\left(M_i^*(t), L^*(t)\right) = (1 - N^*(t))^2 - \frac{4N^*(t)\mu_M\left(\beta + \mu_F\right) M_i^*(t)}{\lambda\nu_A\left[(1-r)(\beta+\mu_F) + r\mu_M\right] K}. \tag{4.15}$$

We define the critical density of *Wolbachia*-infected males by:

$$M_i^{\text{crit}}(t) = \frac{\lambda\nu_A\left[(1-r)(\beta+\mu_F) + r\mu_M\right] K}{4\mu_M(\beta+\mu_F)} \cdot \frac{(1 - N^*(t))^2}{N^*(t)}. \tag{4.16}$$

Using the bounds from (4.7), we have

$$M^*_{i,\min} \le M_i^*(t) \le M^*_{i,\max}.$$

Noting that $\Delta\left(M_i^*(t), L^*(t)\right)$ is strictly decreasing in $M_i^*(t)$, we obtain the following:

- If $M^*_{i,\min} \ge \sup_t M_i^{\text{crit}}(t)$, then $\Delta\left(M_i^*(t), L^*(t)\right) \le 0$ for all t.
- If $M^*_{i,\max} < \inf_t M_i^{\text{crit}}(t)$, then $\Delta\left(M_i^*(t), L^*(t)\right) > 0$ for all t.

The following result establishes the conditions for the solutions of the quadratic Eq (4.12).

Theorem 4.3. *The reduced algebraic Eq (4.12) satisfies the following properties.*

(i) If $\mathcal{N} \le 1$, then Eq (4.12) admits no positive time-dependent solution $x(t) > 0$ for all t.
(ii) If $\mathcal{N} > 1$ and $L^*_{\min} > L^{crit}$, then Eq (4.12) admits no positive time-dependent solution.
(iii) If $\mathcal{N} > 1$, $L^*_{\max} < L^{crit}$, and $M^*_{i,\min} > \sup_t M_i^{crit}(t)$, then Eq (4.12) admits no positive time-dependent solution.
(iv) If $\mathcal{N} > 1$, $L^*_{\max} < L^{crit}$, and $M^*_{i,\max} < \inf_t M_i^{crit}(t)$, then Eq (4.12) admits two positive time-dependent solutions

$$x_\pm(t) = \frac{K}{2N^*(t)}\left[N^*(t) - 1 \pm \sqrt{\Delta(M_i^*(t), L^*(t))}\right] > 0.$$

These time-dependent solutions correspond to positive instantaneous states of the reduced asymptotic algebraic system and should not be interpreted directly as periodic solutions of the full impulsive system.

We now establish the existence of positive periodic solutions for the full impulsive system.

Theorem 4.4. *Assume that $\tau_1 = \tau_2 = \tau$ and that the conditions of Case (iv) of Theorem 4.3 hold. Then System* (4.1) *admits at least one positive non-trivial τ-periodic solution.*

Proof. The proof is divided into three steps.

Step 1: Bounded positively invariant set.
By Theorem 4.1, every solution of system (4.1) with non-negative initial conditions remains non-negative and uniformly bounded for all $t \ge 0$. Therefore, a constant $\delta > 0$ exists such that

$$0 \le A(t),\ M(t),\ F(t),\ F_s(t),\ M_i(t),\ L(t) \le \delta, \qquad \forall t \ge 0.$$

Define

$$\Omega = \left\{(A, M, F, F_s, M_i, L) \in \mathbb{R}^6_+ : 0 \leq A, M, F, F_s, M_i, L \leq \delta\right\}.$$

Then Ω is a nonempty, compact, and convex subset of $\mathbb{R}^6_+$.

Moreover, the non-negative cone $\mathbb{R}^6_+$ is positively invariant under system (4.1). Indeed, for each continuous component of system (4.1), the associated vector field satisfies

$$\frac{dX_i}{dt}\Big|_{X_i=0} \geq 0,$$

for all admissible values of the remaining variables, while the impulsive conditions preserve non-negativity.

Furthermore, the uniform boundedness established in Theorem 4.1 implies that the trajectories cannot leave Ω through its upper boundary. Consequently, we have

$$X(0) \in \Omega \quad \Longrightarrow \quad X(t) \in \Omega, \qquad \forall t \geq 0.$$

Hence, Ω is positively invariant under the semiflow generated by System (4.1).

Step 2: Continuity of the Poincaré operator.

Under the assumption $\tau_1 = \tau_2 = \tau$, system (4.1) defines a τ-periodic impulsive semiflow.

For $t \neq n\tau$, the right-hand side of system (4.1) is continuously differentiable with respect to the state variables and is therefore locally Lipschitz continuous. By the standard theory of impulsive differential equations and the continuous dependence of the solutions on the initial conditions (see, for example, [36]), the solution map depends continuously on the initial conditions.

Define the Poincaré operator

$$\mathcal{P} : \Omega \to \Omega, \quad \mathcal{P}(X_0) = X(\tau; X_0),$$

where $X(\tau; X_0)$ denotes the solution of system (4.1) evaluated at time τ corresponding to the initial condition $X_0 \in \Omega$.

Since the solutions depend continuously on initial conditions, the operator $\mathcal{P}$ is continuous. Furthermore, because Ω is positively invariant,

$$\mathcal{P}(\Omega) \subseteq \Omega.$$

Step 3: Application of Brouwer's fixed point theorem.

Since Ω is a nonempty compact convex subset of $\mathbb{R}^6_+$ and the Poincaré operator

$$\mathcal{P} : \Omega \to \Omega$$

is continuous, Brouwer's fixed point theorem guarantees the existence of at least one fixed point $X^* \in \Omega$ such that $\mathcal{P}(X^*) = X^*$. Equivalently, $X(\tau; X^*) = X^*$, which means that the trajectory issued from X^* is τ-periodic [36, 37].

Finally, since the non-negative cone is positively invariant and the assumptions of Case (*iv*) exclude extinction dynamics, the fixed point X^* corresponds to a positive non-trivial τ-periodic solution.

□

Inspired by Remark 4.2 in [24], we define the release and larvicide concentration thresholds associated with the existence conditions of Theorem 4.3(*iv*):

$$\Lambda^* = \inf_t M_i^{\text{crit}}(t)\,(e^{\mu_i\tau_1} - 1)\,, \qquad l_i^* = L^{\text{crit}}\,(e^{m_2\tau_2} - 1)\,. \tag{4.17}$$

Theorem 4.5. *The following qualitative threshold conditions hold.*

(i) If $\mathcal{N} \leq 1$, then Eq (4.12) admits no positive time-dependent solution $x(t) > 0$.
(ii) If $\mathcal{N} > 1$ and $l_i > l_i^*$, then Eq (4.12) admits no positive time-dependent solution $x(t) > 0$.
(iii) If $\mathcal{N} > 1$, $l_i < l_i^*$, and $\Lambda > \Lambda^*$, then Eq (4.12) admits no positive time-dependent solution $x(t) > 0$.
(iv) If $\mathcal{N} > 1$, $l_i < l_i^*$, and $\Lambda < \Lambda^*$, then the reduced algebraic system admits two positive time-dependent solutions. Thus, system (4.1) *admits at least one positive non-trivial τ-periodic solution.*

Corollary 4.1. *The threshold conditions can equivalently be expressed in terms of intervention periods. Define:*

$$\tau_1^* = \frac{1}{\mu_i}\ln\left(1 + \frac{\Lambda}{\inf_t M_i^{crit}(t)}\right), \qquad \tau_2^* = \frac{1}{m_2}\ln\left(1 + \frac{l_i}{L^{crit}}\right). \tag{4.18}$$

Then:

(i) $\Lambda > \Lambda^*$ if and only if $\tau_1 < \tau_1^*$;
(ii) $l_i > l_i^*$ if and only if $\tau_2 < \tau_2^*$.

Proof. The expressions are obtained by substituting the definitions $\Lambda^* = \inf_t M_i^{\text{crit}}(t)(e^{\mu_i\tau_1} - 1)$ and $l_i^* = L^{\text{crit}}(e^{m_2\tau_2} - 1)$ into the inequalities $\Lambda > \Lambda^*$ and $l_i > l_i^*$, respectively, and solving with respect to τ_1 and τ_2. □

Using Corollary 4.1, the threshold conditions established in Theorem 4.5 can be reformulated as follows.

Theorem 4.6. *(i) If $\mathcal{N} \leq 1$, then Eq (4.12) admits no positive time-dependent solution $x(t) > 0$.*
(ii) If $\mathcal{N} > 1$ and $\tau_2 < \tau_2^*$, then Eq (4.12) admits no positive time-dependent solution $x(t) > 0$.
(iii) If $\mathcal{N} > 1$, $\tau_2 > \tau_2^*$, and $\tau_1 < \tau_1^*$, then Eq (4.12) admits no positive time-dependent solution $x(t) > 0$.
(iv) If $\mathcal{N} > 1$, $\tau_2 > \tau_2^*$, and $\tau_1 > \tau_1^*$, then the reduced algebraic system admits two positive time-dependent solutions. Thus, system (4.1) *admits at least one positive non-trivial periodic solution.*

5. Numerical simulations

This section provides a graphical analysis of various control strategies aimed at assessing the impact of each approach on the mosquito population's dynamics. Both optimal and impulsive control models are solved numerically using the fourth-order Runge–Kutta method. The impulsive system was numerically solved using a hybrid procedure combining continuous integration and discrete updates at impulsive times. Between two consecutive impulses, the differential system was integrated using the MATLAB solver `ode45`. At impulsive instants, the corresponding state variables were instantaneously updated according to the impulsive conditions. For the optimal control problem, the optimality system derived from Pontryagin's maximum principle was solved numerically using a forward–backward sweep algorithm. The state system was integrated forward in time using a fourth-order Runge–Kutta scheme,

while the adjoint system was integrated backward in time. The controls were iteratively updated until convergence was achieved. The parameter values used in the numerical simulations are summarized in Table 3.

Table 3. Parameters values of the mosquito models (3.2) and (4.1).

Parameters	Values	Range of values	References	Units
ϕ	1.5	[0.64, 24.86]	[24, 38]	day^{-1}
ν_A	0.1	[0, 1]	[24, 39]	day^{-1}
K	5000	$\left[10^3, 10^5\right]$	[24, 40, 41]	$--$
μ_A	0.0583	[0, 1]	[24, 40]	day^{-1}
μ_M	1/10	[0.02, 0.2]	[24, 38, 42]	day^{-1}
μ_F	1/7	[0.01, 0.2]	[24, 42, 43]	day^{-1}
β	0.7	–	[24, 38]	day^{-1}
μ_{F_s}	1/10	[1/14, 1/7]	[24]	day^{-1}
r	0.6	[0, 1]	[24, 31, 44]	$--$
μ_i	0.07	[0.005, 0.2]	[24, 31, 38]	day^{-1}
ρ	1	$--$	[24]	af^{-1}
λ	1	$--$	[24]	fa^{-1}

5.1. Numerical simulation of the optimal control model

To evaluate the effectiveness of the optimal control strategies, we conduct numerical simulations under a worst-case scenario, i.e., assuming the wild mosquito population is initially at its non-trivial equilibrium and no *Wolbachia*-infected males are present. Specifically, we assume that at the initial time of intervention ($t = 0$), the wild mosquito population is at its endemic equilibrium, while no *Wolbachia*-infected males have yet been introduced into the system (that is, $M_i(0) = 0$). Following the findings in [24], the positive equilibrium $E_2 = (A^{**}, M^{**}, F^{**}, F_s^{**}, M_i^*)$ of the baseline model (i.e., in the absence of sterile males) is given by:

$$A^{**} = \frac{\mu_M M^{**}}{(1-r)\lambda\nu_A}, \quad M^{**} = \frac{\lambda\nu_A K(1-r)(\mathcal{N}-1)}{\mu_M \mathcal{N}}, \quad M_i^* = 0,$$

$$F^{**} = \frac{r\mu_M M^{**}}{(1-r)(\beta+\mu_F)}, \quad F_s^{**} = \frac{r\mu_M \beta M^{**}}{\mu_{F_s}\left[(1-r)(\beta+\mu_F)+r\mu_M\right]}.$$

According to the parameter values listed in Table 3, the basic offspring number is estimated as $\mathcal{N} \approx 4.0084$. The corresponding equilibrium values are approximately:

- $A^{**} \approx 3.753 \times 10^3$ (aquatic stages),
- $M^{**} \approx 1.501 \times 10^3$ (wild males),
- $F^{**} \approx 2.67 \times 10^2$ (non-ovipositing females),
- $F_s^{**} \approx 1.587 \times 10^3$ (fertilized females), and
- $M_i^* = 0$ (*Wolbachia*-infected males).

To ensure the efficacy of sterile male releases, the upper bound of the control variable $u_2(t)$, representing the release rate of *Wolbachia*-infected males, must exceed the critical release threshold $M_i^{\text{crit}} \approx 1.3298 \times$

10^3, as defined in Section 2 and discussed in [19]. Accordingly, we set:

$$u_{2,\max} = 1.7 \times 10^5, \quad u_{1,\max} = 0.45.$$

These bounds are used in the simulations to determine the optimal control profiles and their impact on the mosquito population's dynamics over the control horizon. Figure 1 illustrates the temporal

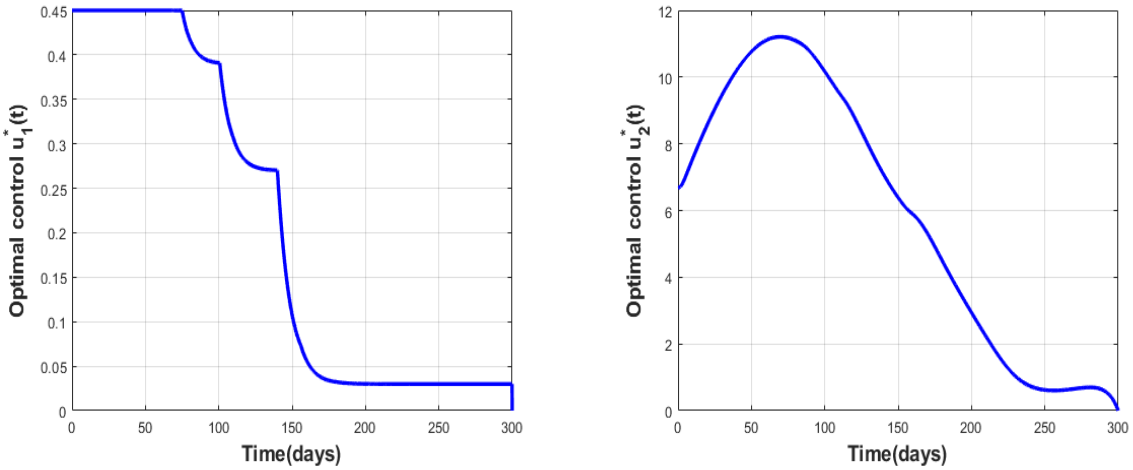

Figure 1. Time dependent profiles of optimal control variables: The larvicide application rate $u_1(t)$ and the *Wolbachia*-infected male release rate $u_2(t)$ for $c_1 = 0.01$ and $c_2 = c_3 = 0.05$.

evolution of the optimal controls $u_1^*(t)$ and $u_2^*(t)$. Here, $u_1^*(t)$ starts at a high level before gradually decreasing and stabilizing at a moderate value, whereas $u_2^*(t)$ begins modestly, reaches an intermediate peak, and then slowly declines. This two-phase profile represents an initially intensive strategy targeting the aquatic population, followed by a gradual increase in reproductive control via *Wolbachia*-infected males. The progressive reduction in both controls mirrors the decline in the target population, thereby minimizing costs while preventing resurgence. Given the low cost associated with fertilized females (c_1), this strategy prioritizes epidemiological effectiveness and optimal resource use, consistent with the principles of optimal control.

Figure 2 shows the optimal control profiles $u_1^*(t)$ and $u_2^*(t)$ for the high social cost associated with fertilized females ($c_1 = 1$). Here, $u_1^*(t)$ remains at its maximum level for a prolonged period before sharply declining to zero, while $u_2^*(t)$ rapidly drops to a very low value. This pattern exemplifies a bang–bang strategy in which both controls are initially applied intensively to reduce larval abundance and reproductive potential. The persistence of $u_1^*(t)$ emphasizes the direct suppression of adult recruitment, whereas the early reduction in $u_2^*(t)$ suggests that sterilization efforts may be relaxed once the aquatic stage is contained. This configuration highlights how high social costs lead to aggressive early intervention followed by progressive relaxation, balancing epidemiological performance and resource allocation efficiency.

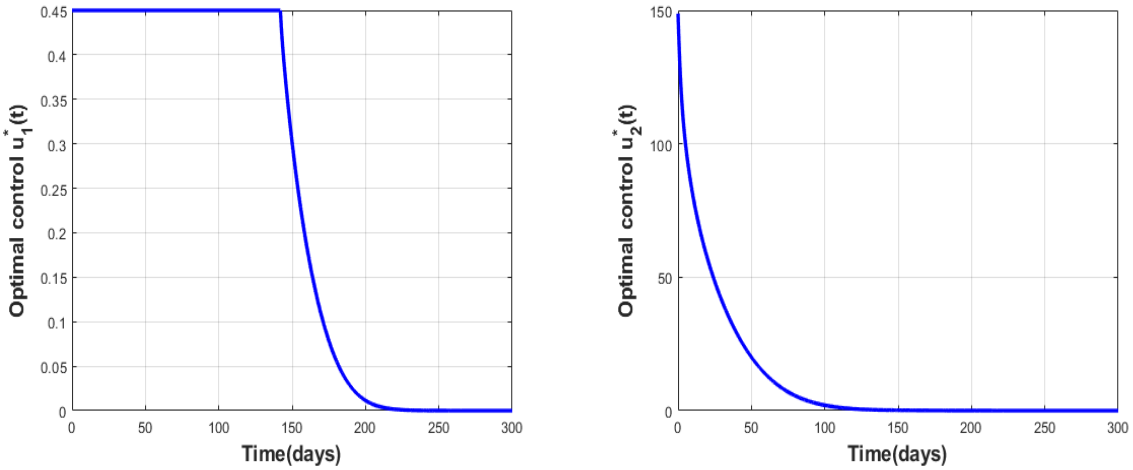

Figure 2. Time dependent profiles of optimal control variables: The larvicide application rate $u_1(t)$ and the *Wolbachia*-infected male release rate $u_2(t)$ for $c_1 = 1$ and $c_2 = c_3 = 0.05$.

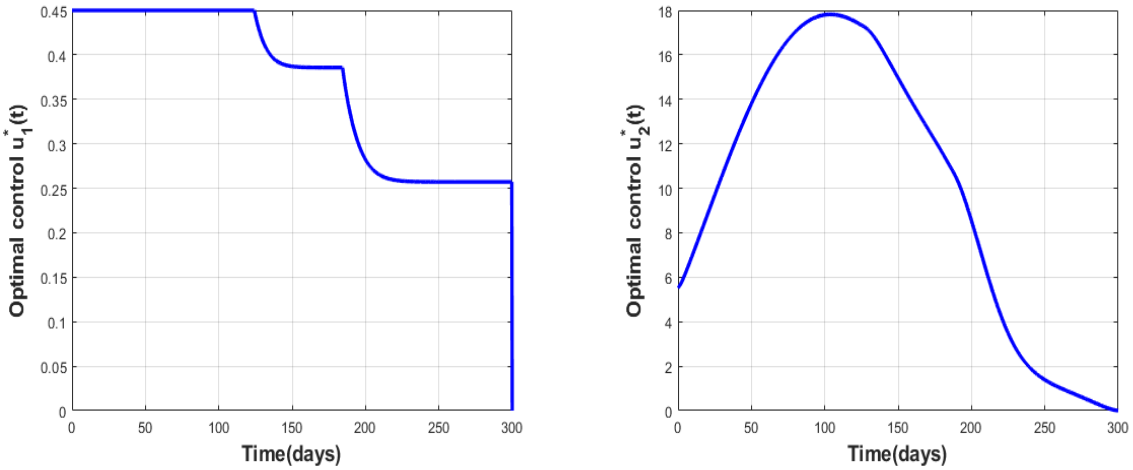

Figure 3. Time dependent profiles of optimal control variables: The larvicide application rate $u_1(t)$ and the *Wolbachia*-infected male release rate $u_2(t)$ for $c_1 = 1$, $c_2 = 5$, and $c_3 = 10$.

Figure 3 presents the optimal controls $u_1^*(t)$ and $u_2^*(t)$ under high intervention costs ($c_2 = 5, c_3 = 10$). Here, $u_1^*(t)$ starts at its maximum, then slightly decreases to stabilize at a moderate value, while $u_2^*(t)$ exhibits an intermediate peak before declining to zero. This pattern highlights the trade-off between epidemiological efficiency and economic feasibility. High intervention costs make intensive control financially impractical, leading to a minimal yet sufficient approach to prevent resurgence while controlling expenses. The temporal spread and stabilization of control levels reflect the quadratic nature of the objective function, which penalizes high costs yet preserves sufficient pressure to maintain suppression.

Remark 5.1. *Figures 1–3 underline the sensitivity of optimal control profiles to the relative costs c_1, c_2, and c_3. This sensitivity demonstrates the economic epidemiological trade-offs inherent in control planning. A low social cost of fertilized females favors an initial larvicide surge followed by reproductive suppression through the use of Wolbachia-infected males. Conversely, a high social*

cost induces sustained larvicide use, emphasizing immature-stage suppression. Rising intervention costs markedly decrease both controls' intensity, underscoring the trade-off between effectiveness and cost feasibility. These variations highlight the value of context-specific cost calibration to generate operationally realistic recommendations.

In the remainder of the numerical simulation of the optimal control model, we examine three distinct scenarios as follows:

- $u_1^* \neq 0$ and $u_2^* = 0$ (red curves),
- $u_1^* = 0$ and $u_2^* \neq 0$ (green curves),
- $u_1^* \neq 0$ and $u_2^* \neq 0$ (blue curves).

The condition $u_i^*(t) \neq 0$ means that the corresponding optimal intervention remains active during the considered time interval.

Table 4. Values of the objective functional J.

Scenarios	Without control	With u_1^* only	With u_2^* only	With u_1^* and u_2^*
J	477,819.8153	109,153.2457	445,101.2457	58,733.3655

Figure 4 compares the evolution of population compartments under four scenarios: No control, larvicide application only, release of *Wolbachia*-infected males only, and combined strategy. In the absence of any intervention, the system remains near its non-trivial equilibrium, with the aquatic compartments $A(t)$, wild males $M(t)$, non-fertilized females $F(t)$, and fertilized females $F_s(t)$ maintaining high levels, confirming the natural persistence of the mosquito population. Larvicide application alone leads to a marked reduction in the aquatic compartment, which gradually affects adult populations, though the reduction in $F_s(t)$ remains partial. Conversely, control using only *Wolbachia*-infected males primarily affects reproduction by decreasing the proportion of fertilized females, while leaving larval recruitment relatively unchanged, which limits its overall effectiveness. The combined strategy clearly stands out, achieving faster and deeper reductions across all compartments, particularly in $F_s(t)$, the primary target of vector control. This superiority arises from the synergistic action of both controls, which simultaneously target recruitment (via u_1^*) and fertility (via u_2^*), thereby more effectively disrupting the mosquito's life-cycle. The associated cost functional values confirm that the integrated strategy offers the best compromise between biological impact and economic cost, outperforming each single-control strategy.

5.2. Numerical analysis of the impulsive model

5.2.1. Numerical illustration of convergence to the trivial periodic solution

In this subsection, we numerically illustrate the convergence of system (4.1) to the trivial periodic solution under the eradication setting. The parameter values are taken from Table 3. We consider the case where the impulsive periods are equal, i.e., $\tau_1 = \tau_2 = 14$ days, which yields the threshold values $\Lambda^* = 181,790$ and $l_i^* = 2.2501$. To satisfy the conditions of Case (ii) of Theorem 4.5, we choose $\Lambda = 5000$ and $l_i = 5$, which exceeds the critical value l_i^*. The initial conditions are set to $A_0 = 3000$, $M_0 = 1000$, $F_0 = 200$, $F_{s0} = 1000$, $M_{i0} = 0$, and $L_0 = 0$. These parameters and initial conditions are used to simulate the system's dynamics over time. Figure 5 illustrates the convergence of the

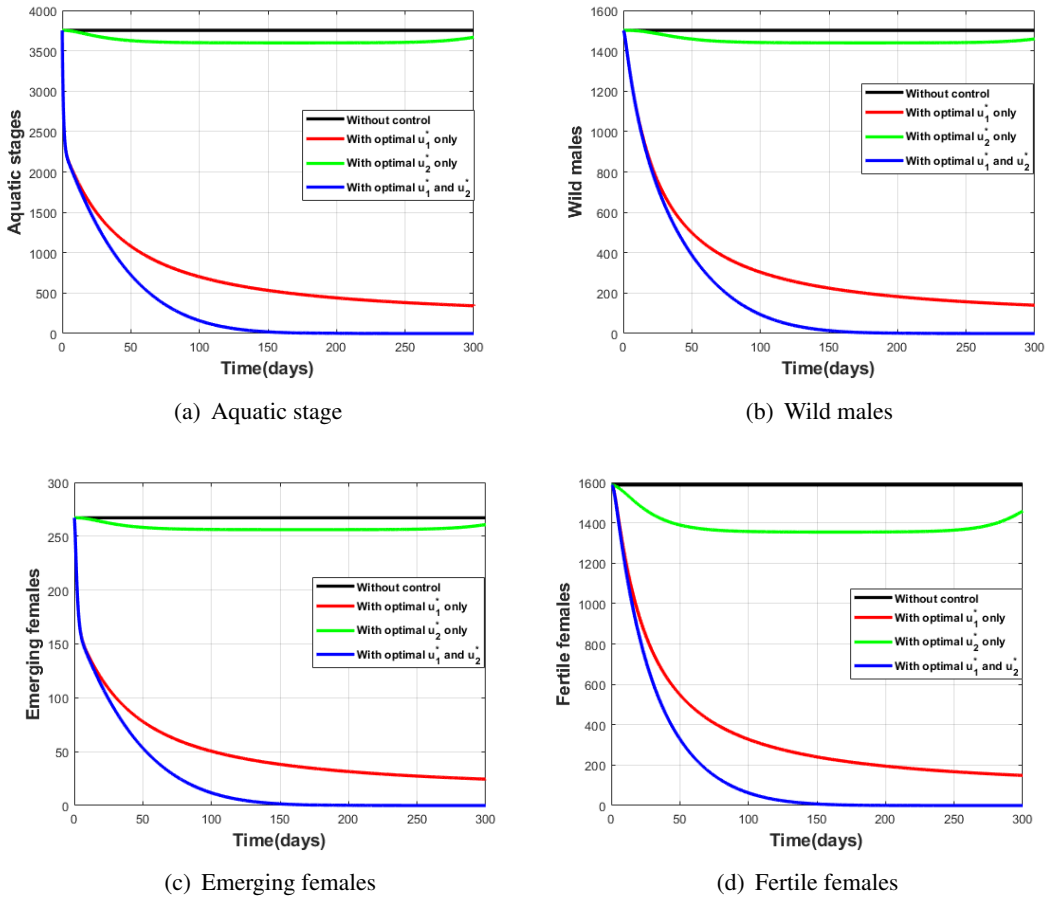

(a) Aquatic stage

(b) Wild males

(c) Emerging females

(d) Fertile females

Figure 4. Comparative effect of three control strategies on the compartments A, M, F, and F_s with $c_1 = c_2 = c_3 = 1$.

impulsive control system to the trivial periodic solution under the eradication setting (Theorem 4.5, Case (ii)). Figure 5(a)–(d) shows that all wild mosquito compartments ($A(t)$, $M(t)$, $F(t)$, $F_s(t)$) decrease to zero. This indicates complete elimination of the wild population. In contrast, Figure 5(e),(f) show that the control variables ($M_i(t)$ and $L(t)$) do not vanish but converge to stable periodic orbits, reflecting the equilibrium between periodic impulsive releases and natural decay. Together, these subfigures numerically demonstrate that a sufficiently strong larvicide application ($l_i > l_i^*$) drives the wild population to extinction while maintaining periodic control interventions.

5.2.2. Numerical analysis of the impulsive control strategy

To assess the effectiveness of time discrete (impulsive) interventions, we conduct a detailed numerical analysis, illustrated in Figures 6–12. These figures examine the system's dynamics under periodic releases of *Wolbachia*-infected male mosquitoes and larvicide treatments. The fixed control intensities are set as $m_1 = 0.6$ for larvicide applications and $m_2 = 0.023$ for male releases. We explore three distinct impulsive control configurations: (i) Male-only releases, (ii) larvicide-only interventions, and (iii) a combined strategy involving both control methods. Each scenario investigates how variation in each

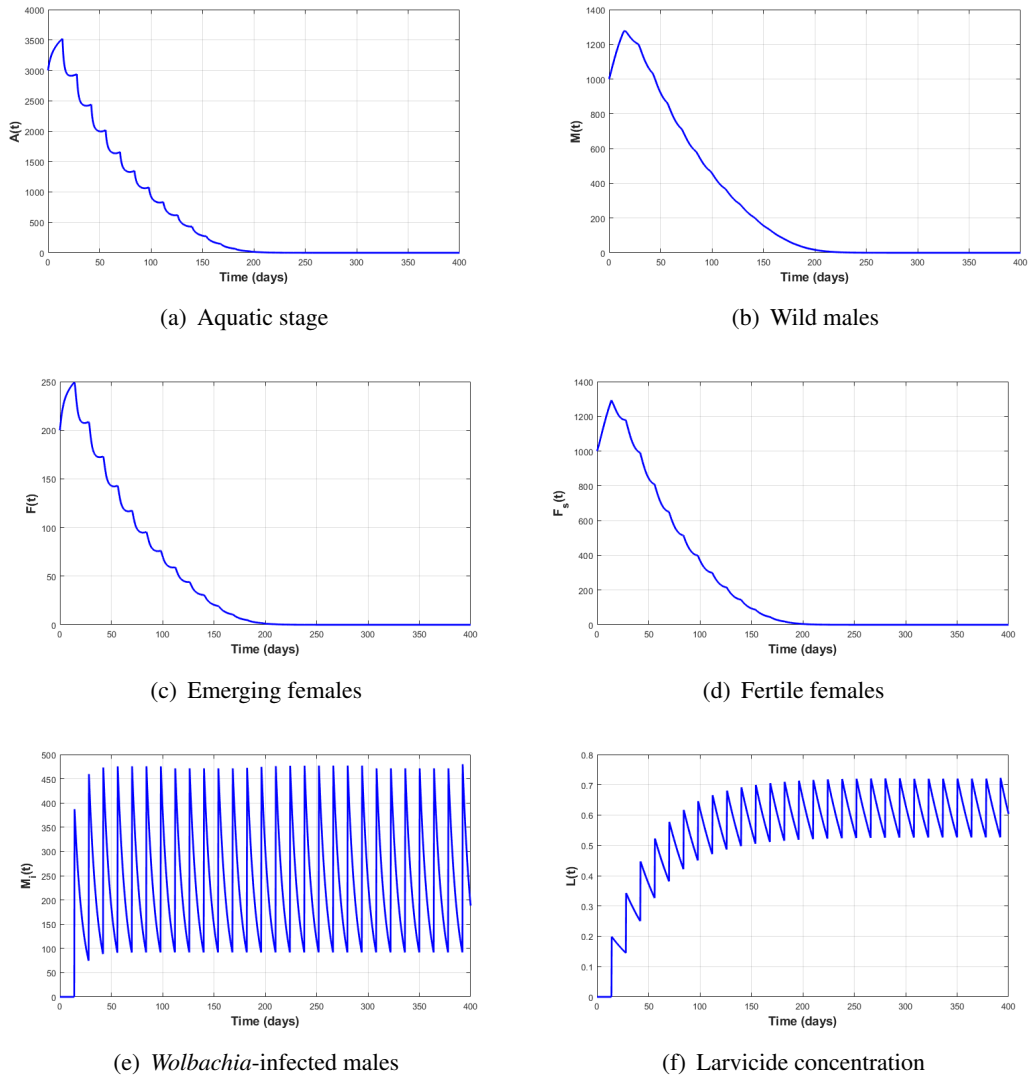

(a) Aquatic stage (b) Wild males

(c) Emerging females (d) Fertile females

(e) *Wolbachia*-infected males (f) Larvicide concentration

Figure 5. Convergence to the trivial periodic solution under the eradication setting.

intervention's frequency or intensity influences key population thresholds and control success.

(i) **Scenario 1:** Release of *Wolbachia*-infected males only, i.e., $\tau_1 \neq 0$ and $\tau_2 = 0$. Under this setup, the release size is set to $N^*(t) = \mathcal{N} = 4.0084$.

(a) *Fixed release size* ($\Lambda = 60,000$) and varying the release period τ_1. Figure 6 presents the corresponding results.

Table 5. Values of Λ^* as a function of τ_1.

τ_1 (days)	7	14	28
Λ^*	197,800	655,990	4,175,800

It is evident that the chosen release size Λ remains below the threshold Λ^* in all cases, suggesting successful suppression.

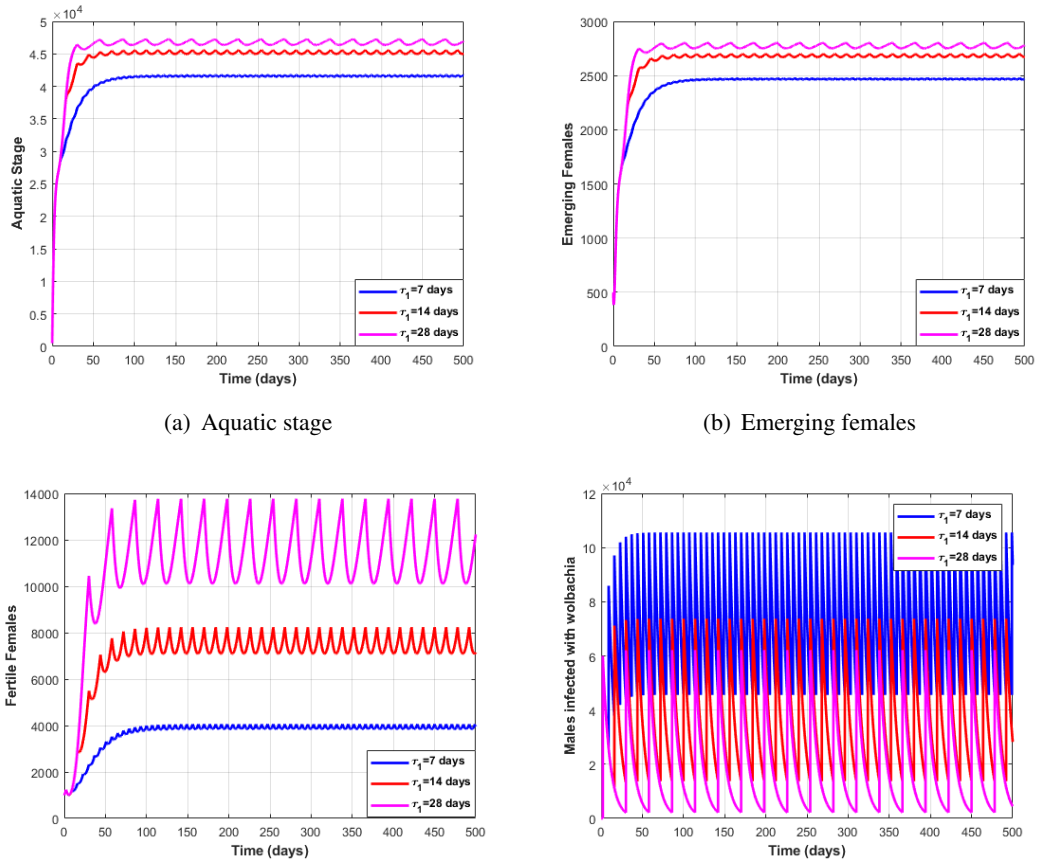

(a) Aquatic stage

(b) Emerging females

(c) Fertile females

(d) *Wolbachia*-infected males

Figure 6. Influence of impulse frequency (τ_1) on the dynamics of the compartments A, F, F_s, and M_i with $\Lambda = 60,000$ and $\tau_2 = 0$.

Figure 6 illustrates the effect of the release period τ_1 ($\tau_1 = 7, 14, 28$ days) on the dynamics of the compartments $A(t)$ (aquatic stages), $F(t)$ (non-fertilized females), $F_s(t)$ (fertilized females), and $M_i(t)$ (infected males) in a scenario involving releases of *Wolbachia*-infected males only, with a fixed release quantity per impulse. It can be observed that more frequent releases ($\tau_1 = 7$ days) maintain a high average density of infected males, characterized by a sawtooth periodic regime of $M_i(t)$ that rapidly reaches a plateau. This strong presence of infected males increases the probability of incompatible matings, resulting in slower growth or even marked attenuation of the $F_s(t)$ and $A(t)$ compartments. Conversely, when the release period is longer ($\tau_1 = 28$ days), infected males remain at low densities between impulses, weakening the control pressure and allowing continuous growth of fertilized females and aquatic stages. These results highlight the crucial role of release frequency in the effectiveness of the control strategy: For a constant release quantity, decreasing τ_1 significantly improves the suppression of the wild population. They confirm the existence of critical thresholds related to τ_1 and Λ, showing that overly spaced releases require larger quantities of infected males to achieve comparable suppression, with direct implications for the operational optimization of SIT campaigns.

(b) Fixed period $\tau_1 = 14$ days and varying the release size Λ. The threshold in this setting is $\Lambda^* = 655,990$. The simulations consider $\Lambda = 60,000$ (blue), $\Lambda = 150,000$ (red), and $\Lambda = 200,000$ (magenta), as illustrated in Figure 7.

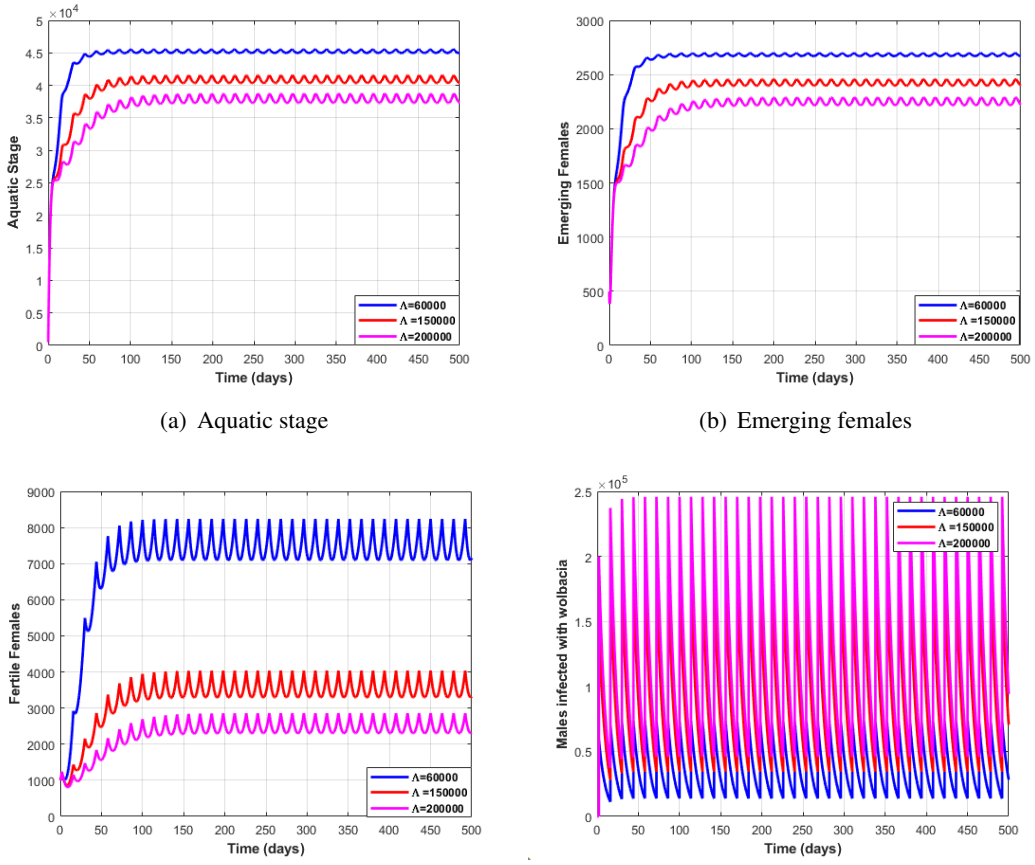

(a) Aquatic stage

(b) Emerging females

(c) Fertile females

(d) *Wolbachia*-infected males

Figure 7. Evolution of compartments A, F, F_s, and M_i for different values of Λ with $\tau_1 = 14$ days and $\tau_2 = 0$.

Figure 7 analyzes the effect of the impulse size Λ ($\Lambda = 60,000,\ 150,000,\ 200,000$) on the dynamics of the compartments $A(t)$ (aquatic stages), $F(t)$ (non-fertilized females), $F_s(t)$ (fertilized females), and $M_i(t)$ (infected males), for a fixed release period of $\tau_1 = 14$ days and in the absence of larvicide. It can be observed that increasing Λ leads to a higher average density of infected males, characterized by larger peaks in $M_i(t)$ and plateaus proportional to the release size. This enhanced presence of *Wolbachia*-infected males slows the growth of the aquatic compartment and results in lower equilibrium levels for $A(t)$ and $F(t)$ as Λ increases. However, for the considered values of Λ, the compartment of fertilized females $F_s(t)$ does not show a significant reduction and remains close to its initial level, indicating the persistence of residual fertility. These results highlight the partial effectiveness of infected male releases when used alone: As long as the impulse size remains below the theoretical critical thresholds Λ^* or M_i^{crit}, the suppressive effect remains insufficient to induce a sustained

decline in $F_s(t)$. The improvement observed for larger values of Λ nevertheless suggests the existence of a flooding threshold, beyond which sexual competition becomes effective, albeit with diminishing marginal returns. This nonlinearity underscores the importance of jointly optimizing release size and frequency, as well as the need for complementary larval recruitment control to achieve significant suppression of the vector population.

(ii) **Scenario 2:** Larvicide treatment only, i.e., $\tau_1 = 0$ and $\tau_2 \neq 0$.

(a) Fixed period $\tau_2 = 7$ days with a varying larvicide intensity l_i. The threshold value is $l_i^* = 1.0347$. Simulated values include $l_i = 0.2$ (blue), $l_i = 0.6$ (red), and $l_i = 0.8$ (magenta) as shown in Figure 8.

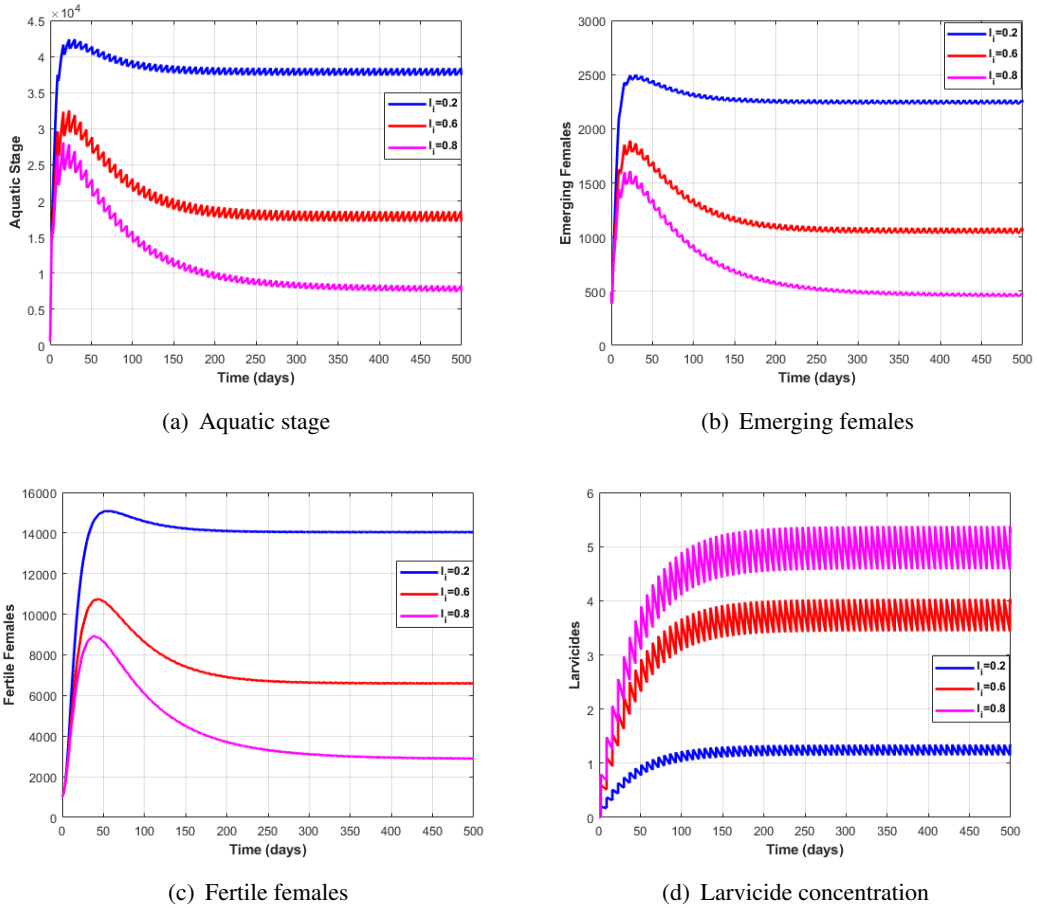

(a) Aquatic stage (b) Emerging females

(c) Fertile females (d) Larvicide concentration

Figure 8. Dynamics of the compartments A, F, F_s, and L under larvicide-only treatment for varying l_i values, with $\tau_1 = 0$ and $\tau_2 = 7$ days.

Figure 8 presents the effect of three larvicide intensities $l_i \in \{0.2, 0.6, 0.8\}$ applied periodically with a period $\tau_2 = 7$ days, in the absence of *Wolbachia*-infected male releases, on the compartments A (aquatic stages), F (non-fertilized females), F_s (fertilized females), and the environmental larvicide concentration $L(t)$. The concentration $L(t)$ follows a sawtooth-like dynamic, characterized by a sharp increase at each impulse followed by an exponential decay between successive applications. As l_i increases, the peaks and temporal average

of $L(t)$ become higher, leading to stabilization at a plateau that is more pronounced for higher application intensities. This rise in the larvicide concentration results in increased mortality in the aquatic compartment, causing the population $A(t)$ to decline rapidly for all values of l_i, with the faster and deeper reduction at higher doses nearly eliminating the aquatic stages for $l_i = 0.8$, while a residual population persists for $l_i = 0.2$. Consequently, non-fertilized females $F(t)$ decrease more gradually but follow the same intensity hierarchy ($0.8 > 0.6 > 0.2$), whereas fertilized females $F_s(t)$ exhibit a much steeper drop, reaching very low levels. These outcomes reflect the direct action of larvicide on the aquatic compartment, the main reservoir for adult population renewal, and an indirect cascading effect on adult compartments via reduced recruitment. When the applied dose allows $L(t)$ to exceed the critical threshold L^{crit} (equivalently, when $l_i > l_i^*$), a sufficiently lethal concentration is maintained between impulses, leading to near-total larval suppression and sustained interruption of adult recruitment. Conversely, for doses below the critical threshold, the system converges to a non-trivial periodic regime characterized by strictly positive mosquito densities, consistent with the theoretical threshold analysis. The persistence of larvicide in the environment, governed by the decay rate m_2, plays a decisive role in overall control efficacy, since the rapid decay of $L(t)$ between applications explains why higher doses produce longer-lasting effects and reduce the necessary treatment frequency. However, the stabilization of the larvicide concentration at high levels underscores the limitations of an exclusively chemical strategy, particularly regarding the ecological risks and the potential selection for resistance in cases of repeated underdosing. This argues in favor of integrated control strategies that combine larvicide with biological or genetic methods to ensure the sustainable suppression of mosquito populations.

(b) Fixed intensity $l_i = 0.2$ and a varying period τ_2. The results are summarized below.

Table 6. Values of l_i^* as a function of τ_2.

τ_2 (days)	5	7	14
l_i^*	0.7219	1.0347	5.3549

The parameter value $l_i = 0.2$ consistently remains beneath the critical threshold across all cases.

Figure 9 illustrates the effect of the larvicide application period $\tau_2 \in \{5, 14, 28\}$ days on the dynamics of the compartments A (aquatic stages), F (non-fertilized females), F_s (fertilized females), and the environmental larvicide concentration $L(t)$, for a fixed application intensity l_i. When the period τ_2 is short, applications are more frequent and the concentration $L(t)$ remains generally high over time, quickly reaching a substantial plateau level. This leads to increased larval mortality and a rapid, deep decline in the aquatic compartment $A(t)$, which is particularly pronounced for $\tau_2 = 5$ days. This reduction in the larval reservoir induces a cascade effect on the adult compartments, resulting in a faster and more pronounced decrease in non-fertilized females $F(t)$ and especially in fertilized females $F_s(t)$, which reach very low levels under frequent applications. As the period τ_2 increases, the impulses become more spaced out, the concentration $L(t)$ declines more between successive applications due to exponential degradation in the environment, and its temporal average decreases, creating vulnerability windows that favor larval survival. In this case, the decline in $A(t)$ is slower

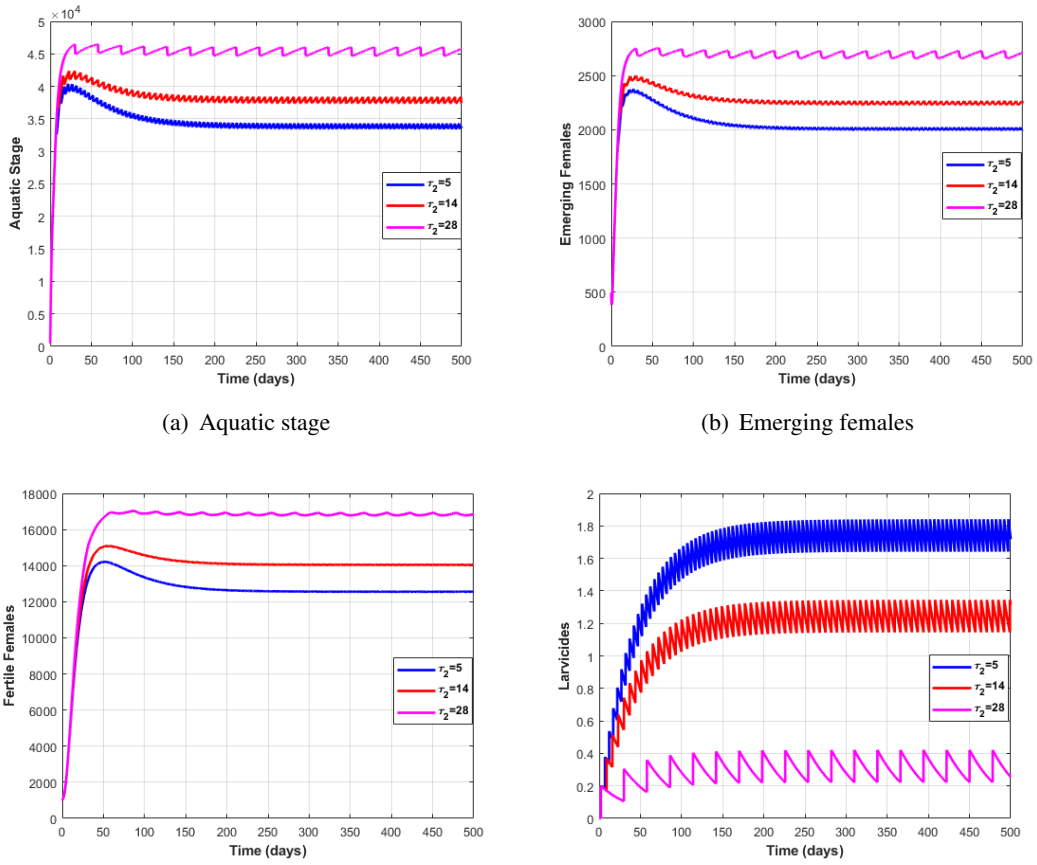

(a) Aquatic stage

(b) Emerging females

(c) Fertile females

(d) Larvicide concentration

Figure 9. Effect of varying the larvicide application period (τ_2) on the compartments A, F, F_s, and L with $l_i = 0.2$ and $\tau_1 = 0$.

and less pronounced, and the compartments $F(t)$ and $F_s(t)$ converge toward periodic regimes characterized by higher densities, as observed for $\tau_2 = 28$ days. These results highlight the decisive role of application frequency in the efficacy of larvicide control, demonstrating that for a given dose, reducing τ_2 helps maintain the larvicide concentration above the lethal threshold for a larger fraction of time and significantly improves the mosquito population's suppression, even when l_i is below the corresponding threshold l_i^*. They also illustrate an important operational trade-off between biological effectiveness and logistical feasibility, as highly frequent applications, though more effective, may be costly or difficult to implement in the field.

(iii) **Scenario 3:** Combined strategy: Release of *Wolbachia*-infected males and larvicide treatment, i.e., $\tau_1 \neq 0$ and $\tau_2 \neq 0$.

(a) *Equal intervention periods*, $\tau_1 = \tau_2$. The table below gives the threshold values.

Table 7. Values of Λ^* and l_i^* for $\tau_1 = \tau_2$.

$\tau_1 = \tau_2$ (days)	7	14	28
Λ^*	24,108	181,790	2,104,800
l_i^*	1.0347	2.2501	5.3549

For simulations, we set $\Lambda = 15,000 < \Lambda^*$ and $l_i = 0.2 < l_i^*$.

Figure 10 illustrates the impact of a synchronized combined strategy integrating larvicide application and releases of *Wolbachia*-infected males, with a common period $\tau_1 = \tau_2 = \tau \in \{7, 14, 28\}$ days, on the dynamics of the compartments A (aquatic stages), M (wild males), F (non-fertilized females), F_s (fertilized females), M_i (infected males), and the larvicide concentration $L(t)$. When the common period is short ($\tau = 7$ days), synchronized impulses generate simultaneous peaks in $M_i(t)$ and $L(t)$, maintaining continuous pressure on both larval recruitment and reproductive success. This results in a rapid and deep decline in the aquatic compartment $A(t)$, a marked reduction in wild males $M(t)$, a sharp drop in non-fertilized females $F(t)$, and, notably, the near long-term elimination of fertilized females $F_s(t)$. For an intermediate period ($\tau = 14$ days), the dynamics remain broadly suppressive, with significant decreases across all compartments, although convergence is slower and the residual densities persist longer. In contrast, when the period becomes long ($\tau = 28$ days), the interventions are too widely spaced to sustain sufficient pressure between impulses: The larvicide concentration $L(t)$ and the density of infected males $M_i(t)$ remain low on average, the aquatic compartment is only partially reduced, and the adult compartments, especially $F_s(t)$, are suppressed only slowly and incompletely. These results highlight the synergy created by synchronizing the two methods: Larvicide reduces the recruitment of immature stages while *Wolbachia*-infected males limit adult fertility. They also demonstrate that, even at moderate intensities ($\Lambda = 15,000$, $l_i = 0.2$), sufficiently frequent and simultaneous applications can lead to substantial reductions in F and F_s. These findings underscore the critical role of frequency and synchronization of the interventions in integrated strategies.

(b) Release more frequently than larvicide, i.e., $\tau_1 < \tau_2$. The thresholds are as follows:

Table 8. Values of Λ^* and l_i^* for $\tau_1 < \tau_2$.

(τ_1, τ_2)	(7, 14)	(14, 21)	(21, 28)
Λ^*	54,817	264,130	865,630
l_i^*	2.2501	3.6778	5.3549

Again, we choose $\Lambda = 15000 < \Lambda^*$ and $l_i = 0.2 < l_i^*$.

Figure 11 presents the system's dynamics under a non-synchronized impulsive combined strategy in which releases of *Wolbachia*-infected males are more frequent than larvicide applications ($\tau_1 < \tau_2$), for three period pairs $(\tau_1, \tau_2) = (7, 14)$, $(14, 21)$, and $(21, 28)$ days, and highlights the evolution of the compartments A (aquatic stages), M (wild males), F (non-fertilized females), F_s (fertilized females), M_i (infected males), and the larvicide concentration $L(t)$. In this configuration, closely spaced impulses of $M_i(t)$ maintain a high average density of infected males, generating quasi-permanent cytoplasmic incompatibility pressure on wild females, while $L(t)$ exhibits more spaced peaks corresponding to less frequent larvicide

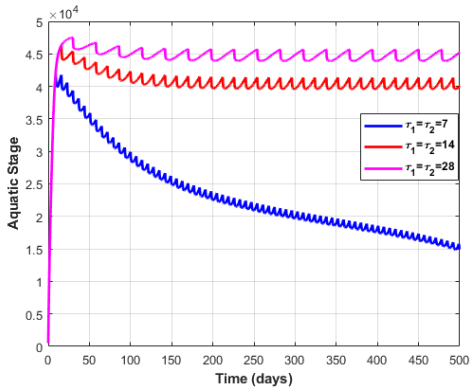

(a) Aquatic stage

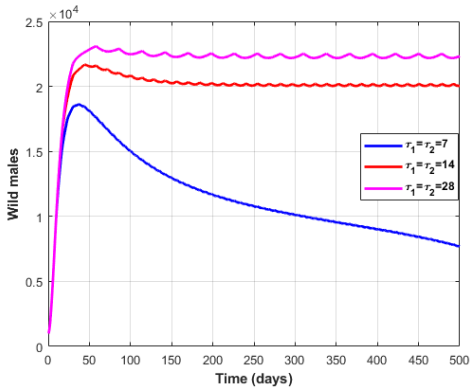

(b) Wild males

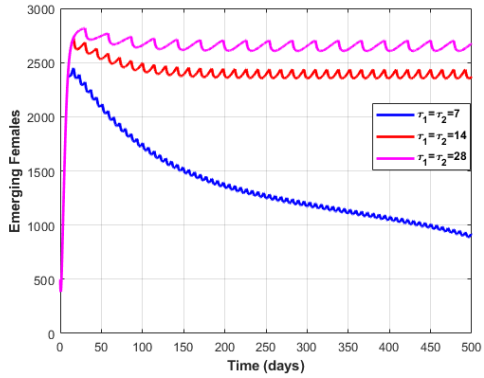

(c) Emerging females

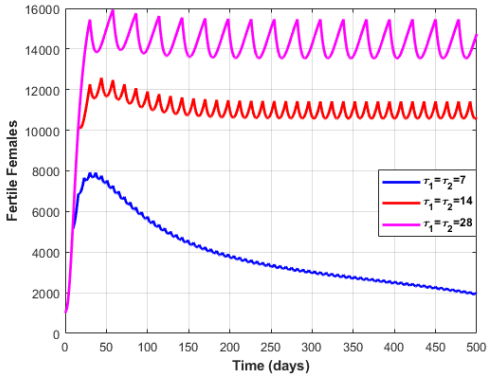

(d) Fertile females

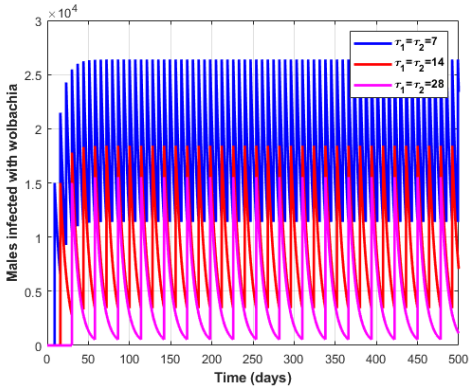

(e) *Wolbachia*-infected males

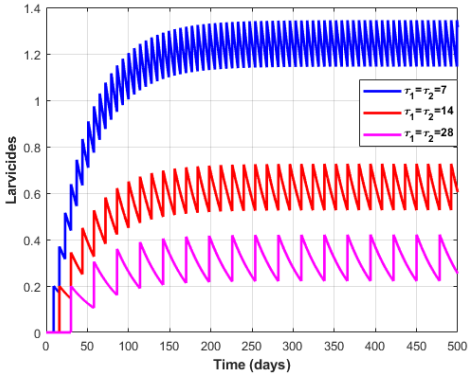

(f) Larvicide concentration

Figure 10. Impulsive combined strategies ($\tau_1 = \tau_2$): Effects on A, M, F, F_s, M_i, and L with $\Lambda = 15,000$ and $l_i = 0.2$.

applications. The simulations show that the aquatic compartment $A(t)$ decreases in all cases, with a reduction that is faster and deeper with a smaller the gap between τ_1 and τ_2, particularly for the pair $(7, 14)$, where larvicide applications, although less frequent, sufficiently limit larval recruitment complementary to adult suppression. Wild males $M(t)$ and non-fertilized

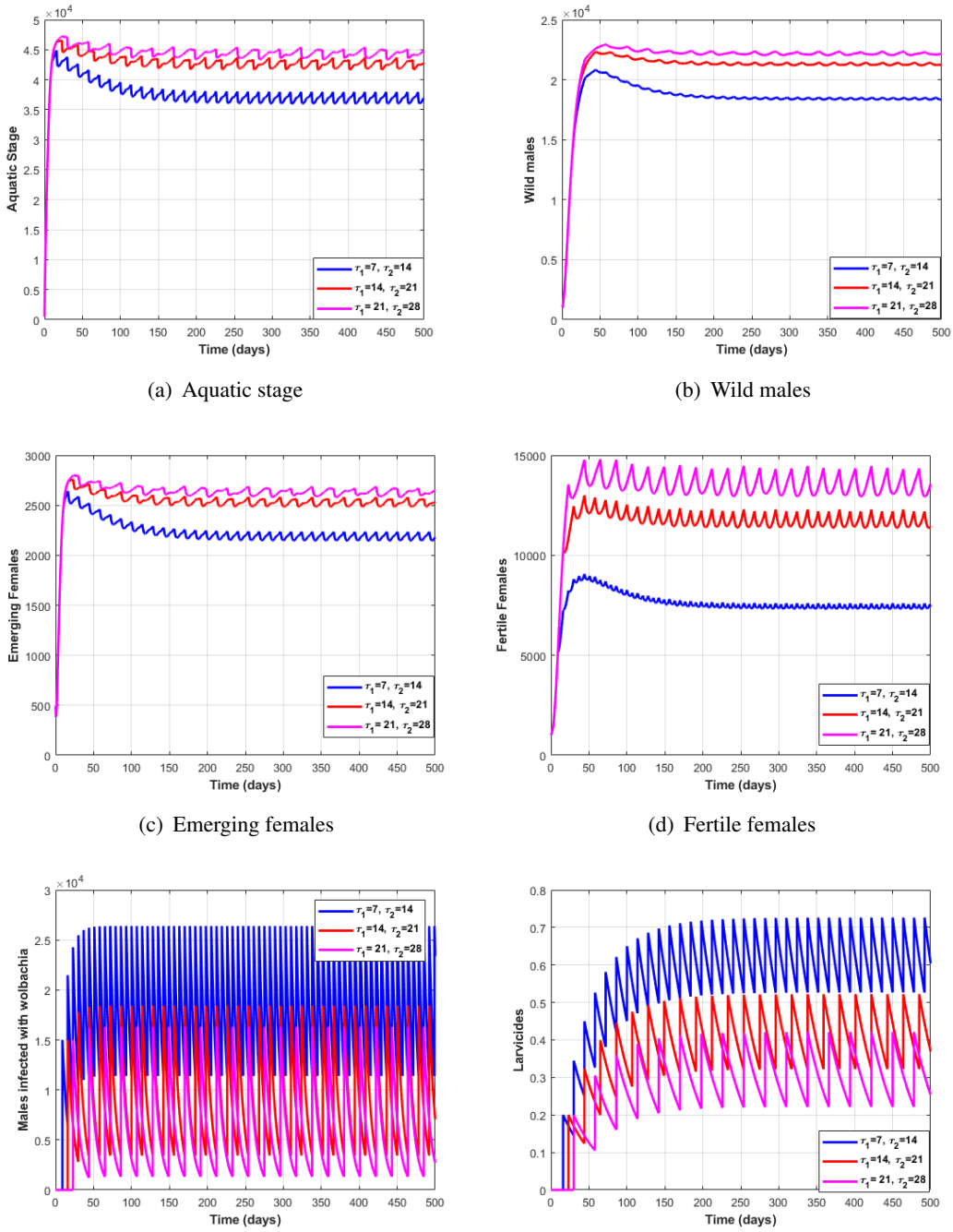

(a) Aquatic stage (b) Wild males

(c) Emerging females (d) Fertile females

(e) *Wolbachia*-infected males (f) Larvicide concentration

Figure 11. Combined strategy with more frequent releases of *Wolbachia*-infected male mosquitoes than larvicide treatments, for $\Lambda = 15,000$ and $l_i = 0.2$.

females $F(t)$ decline gradually, with a more pronounced dynamic for shorter periods, while fertilized females $F_s(t)$ are significantly reduced and reach very low levels when male releases are very frequent, confirming that reducing τ_1 is a decisive lever for suppressing reproduction. The density of infected males $M_i(t)$ converges to a plateau that is higher with a smaller τ_1,

strengthening sexual competition and the probability of incompatible matings, whereas the larvicide concentration $L(t)$ increases stepwise toward a periodic regime whose level depends on τ_2. The best overall performance is achieved for the pair $(\tau_1, \tau_2) = (7, 14)$, where highly frequent male releases compensate for the relative scarcity of larvicide applications and lead to rapid and profound suppression across all compartments, including $F_s(t)$. These results demonstrate that, even with a moderate larvicide dose, increasing the frequency of male releases can optimize control efficacy, making infected males the primary suppression tool and larvicide a supporting mechanism, thereby reducing chemical use while maintaining high effectiveness. They ultimately underscore the importance of balancing the frequencies τ_1 and τ_2 in integrated strategies.

(c) The larvicide is applied more frequently than the release of infected males, i.e., $\tau_1 > \tau_2$. The corresponding threshold values are as follows.

Table 9. Values of Λ^* and l_i^* for $\tau_1 > \tau_2$.

(τ_1, τ_2)	(14, 7)	(21, 14)	(28, 21)
Λ^*	79,950	475,920	1,681,300
l_i^*	1.0347	2.2501	3.6778

These cases are simulated using $\Lambda = 15,000 < \Lambda^*$ and $l_i = 0.2 < l_i^*$, as depicted in Figure 12. Figure 12 considers the inverse configuration of the previous scenarios, in which larvicide applications are more frequent than releases of infected males ($\tau_2 < \tau_1$). In this case, the larvicide concentration $L(t)$ shows closely spaced peaks, reflecting a regular and sustained chemical pressure on the aquatic compartment, while the density of infected males $M_i(t)$ displays more widely spaced impulses, indicating a less continuous presence of *Wolbachia*-infected males in the population. This dynamic leads to a clear decline in the aquatic compartment $A(t)$ and, through a cascade effect, a reduction in the adult compartments $M(t)$, $F(t)$, and $F_s(t)$. However, due to the lower frequency of releases, the proportion of incompatible matings remains limited over large time intervals, resulting in a slower and less pronounced decrease in the fertilized female compartment $F_s(t)$ compared with configurations where male releases are more frequent than larvicide applications. Although the overall treatment effect remains significant, its efficacy in suppressing reproduction is lower than when priority is given to the frequency of male releases. This configuration highlights a clear trade-off between chemical pressure and fertility control: Strengthening larval control strongly reduces the total population, but at the cost of more intensive larvicide use and a more moderate impact on reproductive dynamics. Compared with the other studied strategies, this scenario underscores that the frequency of infected male releases is a decisive lever for maximizing the reduction of $F_s(t)$ and suggests that, from the perspective of long-term effectiveness and environmental sustainability, it is preferable to prioritize frequent releases of *Wolbachia*-infected males, supplemented by more spaced larvicide applications.

Remark 5.2. *Figures 6–12 highlight the decisive role of impulsive parameters, intervention periods, impulse sizes, and control synchronization, in the efficacy of strategies for controlling mosquito populations. Figures 6 and 7 show that in the case of Wolbachia-infected male releases alone, increasing the*

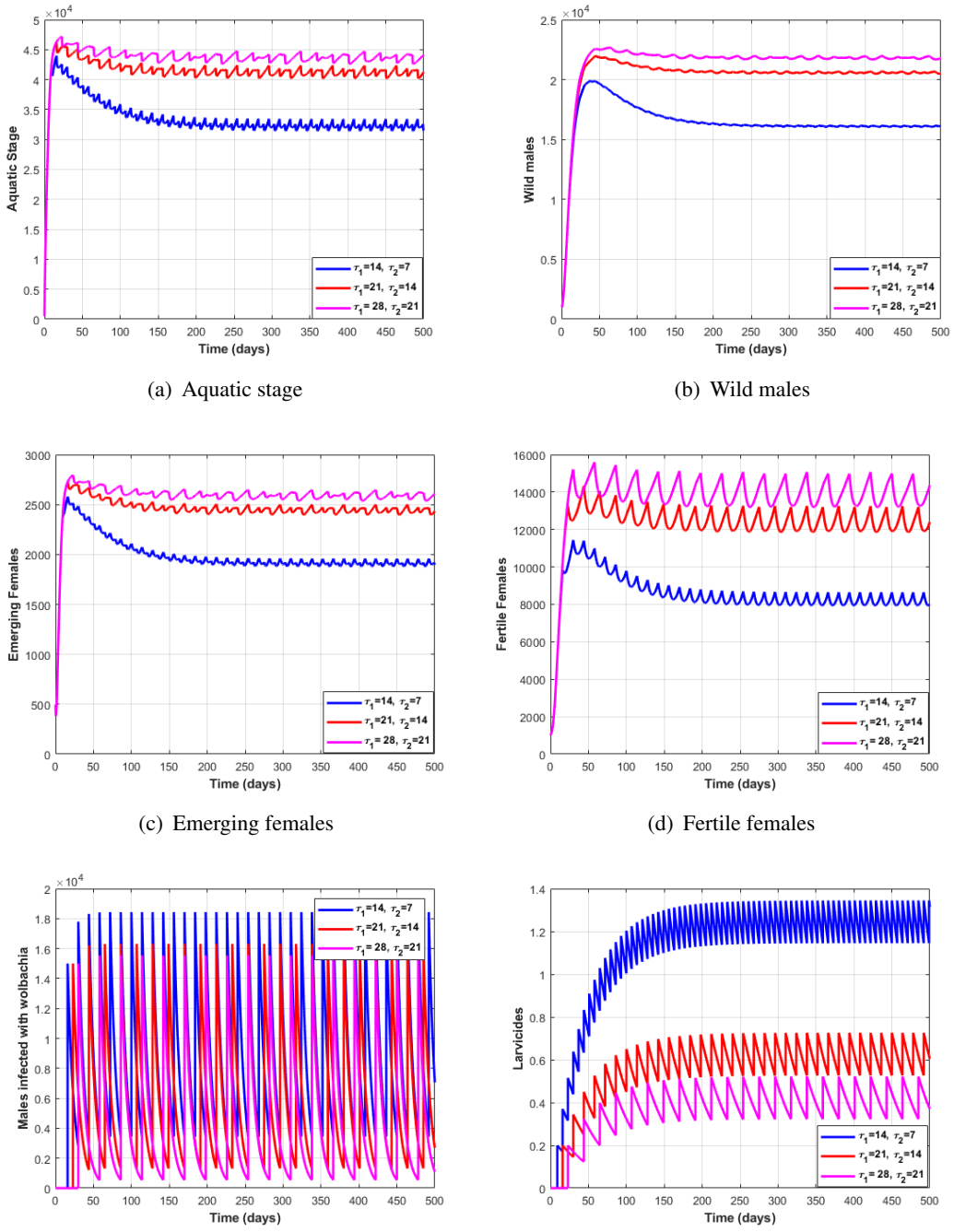

(a) Aquatic stage

(b) Wild males

(c) Emerging females

(d) Fertile females

(e) *Wolbachia*-infected males

(f) Larvicide concentration

Figure 12. Combined strategy with more frequent larvicide treatments than releases for $\Lambda = 15,000$ and $l_i = 0.2$.

frequency or size of impulses improves population suppression, but is still insufficient to sustainably eliminate fertilized females F_s when larval recruitment is not simultaneously controlled, confirming the existence of a critical threshold linked to Λ. Figures 8 and 9 indicate that larvicide alone can induce a marked reduction in compartments, particularly when the intensity and frequency of application

exceed the corresponding critical thresholds, but that exclusive chemical pressure leads to operational and environmental limitations, as well as a risk of residual persistence in cases of underdosing or excessive spacing of applications. Figures 10–12 demonstrate that combined strategies systematically outperform single-control approaches, especially when the interventions are synchronized or when the frequency of male releases is prioritized over that of larvicide. Synchronization of the impulses (Figure 10) maximizes the synergistic effect between larval recruitment reduction and fertility suppression, while Figures 11 and 12 reveal that an imbalance in the intervention frequencies profoundly alters overall efficacy: More frequent male releases than larvicide applications promote rapid and sustained suppression of F_s, whereas the opposite situation, although biologically effective, relies more heavily on increased chemical pressure. Taken together, these figures confirm that optimal efficacy depends less on the isolated intensity of each control than on a fine calibration of the frequencies, amplitudes, and their temporal coordination, consistent with the analytical thresholds of the impulsive model, and underscore the operational relevance of flexible integrated strategies adapted to local logistical and economic constraints.

Remark 5.3. *The multiplicity of nontrivial periodic solutions established in Theorems 4.5 and 4.6 is derived analytically from the threshold conditions and discriminant analysis. A complete numerical verification of two distinct periodic attractors would require an exhaustive exploration of the initial conditions and basins of attraction, which is beyond the main scope of this work. Therefore, the numerical section is primarily intended to illustrate the comparative efficiency of the proposed control strategies rather than to investigate the complete bifurcation structure and attraction basins of the impulsive system. Such a detailed numerical investigation is left for future research.*

6. Conclusions

This study has developed a comprehensive mathematical modeling framework for mosquito vector control by integrating both optimal continuous and impulsive intervention strategies. Extending the foundational work of [24], which considered constant releases of *Wolbachia*-infected male mosquitoes, we propose a dual control approach that combines larvicide application with the release of infected males to enhance the effectiveness of mosquito population reduction.

In the first part of the study, we developed an optimal control model formulated through a system of ODEs. This model incorporates continuous larvicide application and continuous release of *Wolbachia*-infected males. The objective function was designed to minimize the number of fertilized female mosquitoes recognized as the primary vectors of vector-borne diseases while simultaneously reducing the overall cost associated with control measures. Both the analytical and numerical results confirmed the effectiveness and cost-efficiency of this integrated continuous strategy. The second part of the study introduced an impulsive control model to evaluate the impact of periodic interventions. This model allowed us to assess the system's behavior under discrete time applications of larvicides and releases of infected males. We identified key threshold conditions, denoted by Λ^* and l_i^*, that must be met to ensure the suppression of the wild mosquito population. Numerical simulations demonstrated that impulsive strategies, when properly timed and implemented, can achieve similar levels of population suppression as continuous interventions. In particular, the combined strategy was most effective when the frequency of *Wolbachia*-infected male releases exceeded that of larvicide applications, while remaining within feasible operational limits. Overall, our findings underscore the potential of integrated vector

management strategies that harmonize biological and chemical control methods. The combination of larvicides and sterile male releases provides a complementary approach that enhances vector suppression, limits reproductive capacity, and offers operational flexibility. Such strategies are particularly promising in the context of resistance management and environmentally sustainable vector control.

The critical threshold M_i^{crit} derived in this study should be interpreted as a mathematical condition for achieving a sustained reduction in the target wild mosquito population within the proposed modeling framework. Our objective is not to advocate for the indiscriminate eradication of mosquito species, but rather to contribute to the reduction of vector populations responsible for disease transmission. It is worth noting that *Wolbachia*-based control strategies are generally considered to be more specific and ecologically less detrimental than certain conventional chemical methods, as they primarily target the vector population without directly affecting a broad range of non-target organisms. Nevertheless, we acknowledge that ecological implications and biodiversity concerns are important considerations that merit further investigation. Future studies should aim to incorporate explicit ecological interactions between species into the modeling framework to better assess the potential impacts of vector control strategies on ecosystem dynamics.

Future work should focus on extending the model to incorporate seasonal and environmental variability, as mosquitoe's life-cycles and transmission dynamics are highly sensitive to climatic factors such as temperature and rainfall. Integrating seasonality would enhance the model's applicability to real-world settings and support the development of adaptive, time-sensitive intervention programs tailored to local ecological and epidemiological conditions. One limitation of the present study is that the larvicide lethality rate was assumed to remain constant throughout the study period. However, in real mosquito populations, prolonged exposure to insecticides may lead to resistance phenomena and reduced larvicide effectiveness over time. Incorporating time-dependent insecticide resistance into the model would therefore constitute an important and biologically relevant direction for future research. Furthermore, while the present study focused exclusively on larvicides as the chemical intervention targeting aquatic stages, other strategies such as mechanical destruction of breeding sites, biological methods, and environmental measures could also be considered. Incorporating these alternative interventions into the modeling framework constitutes another promising direction for future research. Additionally, coupling the entomological model with a host–vector transmission framework would allow for evaluation of disease incidence and the direct epidemiological benefits of control strategies.

Use of AI tools declaration

The authors declare they have not used artificial intelligence (AI) tools in the creation of this article.

Conflict of interest

The authors declare there is no conflict of interest.

References

1. M. A. Marzaleh, M. H. Ainvand, Strategic solutions to overcome emerging public health challenges with emphasis on vector-borne diseases (VBDs), *EXCLI J.*, **23** (2024), 1353. https://doi.org/10.17179/excli2024-7695
2. *World Health Organization*, Updated WHO guidance for controlling vector-borne diseases through indoor residual spraying, 2024. Available from: https://www.who.int/news-room/fact-sheets/detail/indoor-residual-spraying.
3. B. M. de Carvalho, L. P. Perez, B. F. A. de Oliveira, L. da S. V. Jacobson, M. A. Horta, A. Sobral, et al., Vector-borne diseases in Brazil: climate change and future global warming scenarios, *Sustain. Debate*, **11** (2020), 361–404. https://doi.org/10.18472/SustDeb.v11n3.2020.33985
4. S. Kezeta-Bondja, C. S. Wondji, R. Djidjou-Demasse, Optimizing insecticide deployment strategies to delay quantitative resistance in mosquito populations, *J. Math. Biol.*, **92** (2026), 37. https://doi.org/10.1007/s00285-026-02343-z
5. A. M. Pulecio-Montoya, L. E. López-Montenegro, J. Y. Medina-García, Description and analysis of a mathematical model of population growth of *Aedes aegypti*, *J. Appl. Math. Comput.*, **65** (2021), 335–349. https://doi.org/10.1007/s12190-020-01394-9
6. A. E. Flores, J. A. Davila-Barboza, A. E. Juache-Villagrana, Insecticide resistance and vector control, *Trop. Med. Infect. Dis.*, **11** (2026), 33. https://doi.org/10.3390/tropicalmed11010033
7. A. Kaboré, W. Birba, B. Sangaré, Mathematical modeling of malaria transmission global dynamics: taking account the release of *Wolbachia*-infected male mosquitoes, *Math. Comput. Model. Dyn. Syst.*, **31** (2025), 1–37. https://doi.org/10.1080/13873954.2025.2500439
8. K. Tiley, L. Yakob, K. O'Reilly, O. Brady, Mathematical modelling of *Wolbachia* replacement in Aedes aegypti for dengue control: a scoping review, *Proc. Biol. Sci.*, **293** (2026), 20252952-.ISSN 0962-8452. https://doi.org/10.1098/rspb.2025.2952
9. I. D. Velez, A. Uribe, J. Barajas, S. Uribe, S. Angel, J. D. Suaza-Vasco, et al., Large-scale releases and establishment of wMel *Wolbachia* in *Aedes aegypti* mosquitoes throughout the cities of Bello, Medellín and Itagüí, Colombia, *PLoS Negl. Trop. Dis.*, **17** (2023), e0011453. https://doi.org/10.1371/journal.pntd.0011642
10. L. A. Moreira, J .A. Jeffery, A *Wolbachia* symbiont in *Aedes aegypti* limits infection with dengue, chikungunya, and plasmodium, *Cell*, **139** (2009), 1268–1278. https://doi.org/10.1016/j.cell.2009.11.042
11. A. Utarini, C. Indriani, R. A. Ahmad, W. Tantowijoyo, E. Arguni, M. R. Ansari, et al., Efficacy of *Wolbachia*-infected mosquitoes in dengue control, *N. Engl. J. Med.*, **384** (2021), 2177–2186. https://doi.org/10.1056/NEJMoa2030243
12. K. P. Padilha, G. A. Garcia, R. Teles-de-Freitas, F. J. Gnonhoue, M. R. David, J. Corrêa-Antônio, et al., Wolbachia introgression in Rio de Janeiro remains at sub-optimal levels 30 months after its crash: challenges in the sustainability of wMel interventions for dengue control, *bioRxiv*, 2025. https://doi.org/10.1101/2025.07.29.667468

13. A. Diabaté, B. Sangaré, O. Koutou, Optimal control analysis of a COVID-19 and tuberculosis (TB) co-infection model with an imperfect vaccine for COVID-19, *SeMA J.*, **81** (2023), 429–456. https://doi.org/10.1007/s40324-023-00330-8

14. A. A. Momoh, D. Déthié, N. S. Isah, W. J. Dekera, J. A. Adewale, A. I. Michael, Mathematical modeling and optimal control of a vector-borne rice yellow mottle virus disease, *Int. J. Dyn. Control*, **12** (2024), 600–618. https://doi.org/10.1007/s40435-023-01188-4

15. N. M. Ferguson, D. T. H. Kien, H. Clapham, R. Aguas, V. T. Trung, T. N. B. Chau, et al., Modeling the impact on virus transmission of *Wolbachia*-mediated blocking of dengue virus infection of Aedes aegypti, *Sci. Transl. Med.*, **7** (2015), 279ra37. https://doi.org/10.1126/scitranslmed.3010370

16. S. Ullah, M.F. Khan, S. A. A. Shah, M. Farooq, M. A. Khan, M. bin Mamat Optimal control analysis of vector-host model with saturated treatment, *Eur. Phys. J. Plus*, **135** (2020), 839. https://doi.org/10.1140/epjp/s13360-020-00855-1

17. L. Multerer, T. Smith, N. Chitnis, Modeling the impact of sterile males on an Aedes aegypti population with optimal control, *Math. Biosci.*, **311** (2019), 91–109. https://doi.org/10.1016/j.mbs.2019.03.003

18. R. C. A. Thomé, H. M. Yang, L. Esteva, Optimal control of *Aedes aegypti* mosquitoes using the sterile insect technique and insecticides, *Math. Biosci.*, **223** (2010), 12–23. https://doi.org/10.1016/j.mbs.2009.08.009

19. P. A. Bliman, D. Cardona-Salgado, Y. Dumont, O. Vasilieva, Optimal control approach for implementation of sterile insect techniques, *J. Math. Sci.*, **279** (2024), 607–622. https://doi.org/10.1007/s10958-024-07042-y

20. F. A. Basir, J. Chowdhury, D. F. M. Torres, Dynamics of a double-impulsive control model of integrated pest management using perturbation methods and floquet theory, *Axioms*, **12** (2023), 391. https://doi.org/10.3390/axioms12040391

21. J. Dianavinnarasi, R. Raja, J. Alzabut, M. Niezabitowski, O. Bagdasar, Controlling *Wolbachia* transmission and invasion dynamics among *Aedes aegypti* population via impulsive control strategy, *Symmetry*, **13** (2021), 434. https://doi.org/10.3390/sym13030434

22. Y. Li, X. Liu, An impulsive model for *Wolbachia*-infection control of mosquito-borne diseases with general birth and death rate functions, *Nonlinear Anal. Real World Appl.*, **37** (2017), 412–432. https://doi.org/10.1016/j.nonrwa.2017.03.003

23. L. Wang, L. Chen, J.J. Nieto, The dynamics of an epidemic model for pest control with impulsive effect, *Nonlinear Anal. Real World Appl.*, **11** (2010), 1374–1386. https://doi.org/10.1016/j.nonrwa.2009.02.027

24. A. Kaboré, B. Sangaré, B. Traoré, Mathematical model of mosquito population dynamics with constants and periodic releases of *Wolbachia*-infected males, *Appl. Math. Sci. Eng.*, **32** (2024), 2372581. https://doi.org/10.1080/27690911.2024.2372581

25. X. Ma, Z. Li, L. Cai, How to block the reinvasion of mosquito populations using the sterile insect technique? insights from modelling strategic barrier, *J. Appl. Math. Comput.*, **72** (2026), 89. https://doi.org/10.1007/s12190-025-02729-0

26. P. I. Howell, B. G. J. Knols, Male mating biology, *Malar. J.*, **8** (2009), S8. https://doi.org/10.1186/1475-2875-8-S2-S8
27. A. F. Filippov, *Differential Equations with Discontinuous Righthand Sides: Control Systems*, Springer Science Business Media, 2013.
28. W. Fleming, R. Rishel, Deterministic and stochastic optimal control, *Appl. Math.*, 1975. https://doi.org/10.1007/978-1-4612-6380-7
29. B. Sangaré, Contribution à la modélisation mathématique en épidémiologie et en écologie et à la résolution numérique des EDP évolutives, *Université Franche-Comté*, 2023.
30. S. Lenhart, J. T. Workman, *Optimal Control Applied to Biological Models*, Chapman and Hall/CRC, 2007.
31. Y. Dumont, I. Yatat–Djeumen, Sterile insect technique with accidental releases of sterile females. impact on mosquito-borne diseases control when viruses are circulating, *Math Biosci.*, **343** (2022), 108724. https://doi.org/10.1016/j.mbs.2021.108724
32. I. Stamova, G. T. Stamov, *Applied Impulsive Mathematical Models*, Cham, Switzerland: Springer, 2016.
33. Y. Pang, S. Wang, Dynamic analysis of the *Wolbachia*-infected male mosquitoes model by pulsed release, *Adv. Appl. Math.*, **10** (2021), 3505–3517. https://doi.org/10.12677/AAM.2021.1010370
34. Y. Pang, S. Wang, S. Liu, Dynamics analysis of stage-structured wild and sterile mosquito interaction impulsive model, *J. Biol. Dyn.*, **16** (2022), 464–479. https://doi.org/10.1080/17513758.2022.2079739
35. C. A. Klausmeier, Floquet theory: a useful tool for understanding nonequilibrium dynamics, *Theor. Ecol.*, **1** (2008), 153–161. https://doi.org/10.1007/s12080-008-0016-2
36. R. Tan, Z. Liu, R. A. Cheke, Periodicity and stability in a single-species model governed by impulsive differential equation, *Appl. Math. Modell.*, **36** (2012), 1085–1094. https://doi.org/10.1016/j.apm.2011.07.056
37. J. Á. Cid, J. Mawhin, The Brouwer fixed point theorem and periodic solutions of differential equations, *J. Fixed Point Theory Appl.*, **25** (2023), 25–38. https://doi.org/10.1007/s11784-022-01023-x
38. M. Strugarek, H. Bossin, Y. Dumont, On the use of the sterile insect release technique to reduce or eliminate mosquito populations, *Appl. Math. Modell.*, **68** (2018), 443–470. https://doi.org/10.1016/j.apm.2018.11.026
39. M. Huang, X. Song, J. Li, Modelling and analysis of impulsive releases of sterile mosquitoes, *J. Biol. Dyn.*, **11** (2016), 147–171. https://doi.org/10.1080/17513758.2016.1254286
40. N. Hamdan, A. Kilicman, Mathematical modelling of dengue transmission with intervention strategies using fractional derivatives, *Bull. Math. Biol.*, **84** (2022), 138. https://doi.org/10.1007/s11538-022-01096-2
41. E. Iboi, A. Gumel, J. Taylor, Mathematical modeling of the impact of periodic release of sterile male mosquitoes and seasonality on the population abundance of malaria mosquitoes, *J. Biol. Syst.*, **28** (2020), 277–310. https://doi.org/10.1142/S0218339020400033

42. M. L. M. Manyombe, J. Mbang, B. Tsanou, S. Bowong, J. Lubuma, Mathematical analysis of a spatiotemporal model for the population ecology of anopheles mosquito, *Math. Methods Appl. Sci.*, **43** (2020), 3524–3555. https://doi.org/10.1002/mma.6136

43. J. Himanshu, A. K. Sinha, Modeling the effect of *Wolbachia* to control malaria transmission, *Expert Syst. Appl.*, **221** (2023), 119769. https://doi.org/10.1016/j.eswa.2023.119769

44. H. Hughes, N. F. Britton, Modeling the use of *Wolbachia* to control dengue fever transmission, *Bull. Math. Biol.*, **75** (2013), 796–818. https://doi.org/10.1007/s11538-013-9835-4

AIMS Press